

Parvoviruses: structure and infection

Sujata Halder[†], Robert Ng[‡] & Mavis Agbandje-McKenna^{*}

Department of Biochemistry & Molecular Biology, Center for Structural Biology, The McKnight Brain Institute, College of Medicine, 1600 SW Archer Road, PO Box 100245, University of Florida, Gainesville, FL 32610, USA

*Author for correspondence: Fax: +1 352 392 3422 ■ mckenna@ufl.edu

[†]Authors contributed equally

Parvoviruses package a ssDNA genome. Both nonpathogenic and pathogenic members exist, including those that cause fetal infections, encompassing the entire spectrum of virus phenotypes. Their small genomes and simple coding strategy has enabled functional annotation of many steps in the infectious life cycle. They assemble a multifunctional capsid responsible for cell recognition and the transport of the packaged genome to the nucleus for replication and progeny virus production. It is also the target of the host immune response. Understanding how the capsid structure relates to the function of parvoviruses provides a platform for recombinant engineering of viral gene delivery vectors for the treatment of clinical diseases, and is fundamental for dissecting the viral determinants of pathogenicity. This review focuses on our current understanding of parvovirus capsid structure and function with respect to the infectious life cycle.

Parvoviridae: classification & structure

The *Parvoviridae* family consists of small, non-enveloped icosahedral viruses that package a linear, ssDNA genome of approximately 5000 bases within an approximately 260 Å capsid [1]. Based on the host range, these viruses are divided into two subfamilies: *Parvovirinae* and *Densovirinae* [2]. The *Parvovirinae*, which infect vertebrates, are further subdivided into five genera: *Amdovirus*, *Bocavirus*, *Dependovirus*, *Erythrovirus* and *Parvovirus*, based on genome architecture and phylogenetic analysis. Members of the *Densovirinae* (subdivided into four genera: *Iteravirus*, *Brevidensovirus*, *Densovirus* and *Pefudensovirus*) infect only insects and arthropods. Due to the limited information on the *Densovirinae* with respect to functional annotation of the capsid structure, this review will focus on members of the *Parvovirinae*.

The type species of each of the *Parvovirinae* genera are: *Amdovirus*: Aleutian mink disease virus (ADV); *Bocavirus*: bovine parvovirus (BPV1); *Dependovirus*: adeno-associated virus serotype 2 (AAV2); *Erythrovirus*: human parvovirus B19V (B19V); and *Parvovirus*: minute virus of mice (MVM) [2]. Members of the *Dependovirus* genus rely on coinfection with a complex helper virus (such as adenovirus [Ad] or HSV) for productive infection (except for duck and goose parvoviruses, which do not require a helper). The other genera contain viruses that can replicate independently of helper virus function, and are thus referred to as autonomous parvoviruses [3–5]. The common genomic structure of parvoviruses consists of two open reading frames

(ORFs) flanked by palindromic sequences (120 to ~550 nucleotides in length) that fold into hairpin structures and are essential for replication. The terminal hairpins may be part of an inverted terminal repeat (e.g., members of the *Dependovirus* and *Erythrovirus* genera) or may be different in sequence and structure (e.g., members of the *Parvovirus* genus). The 5' end ORF (*rep* or *ns*) encodes nonstructural proteins (referred to as Rep in the dependoviruses and NS in the autonomous parvoviruses) that are important for genome replication and packaging, while the 3' ORF (*cap*) encodes structural viral proteins (VPs) that assemble the capsid [6]. Members of the *Bocavirus* genus have a third ORF between *rep* and *cap* that codes for a non-structural protein, NP-1, required for genome replication [7,8].

The number of VPs encoded by the *cap* gene and used to assemble the capsid differs between members of the *Parvovirinae*. The dependoviruses (AAVs) contain VP1, VP2 and VP3 formed by alternative mRNA splicing of the transcript and alternative translation initiation codon usage, whereas the autonomous parvoviruses are assembled from two to three VPs translated from alternatively spliced mRNAs or alternative codon usage [6,7,9,10]. For the *Parvovirus* genus, a VP3 is generated by post-translational cleavage of approximately 25 amino acids from the N-terminus of VP2 following genome packaging [6]. The bocavirus BPV1 contains VP4 generated by post-translational cleavage of VP3 [9,10]. Thus, ADV and B19V contain only VP1 and VP2; AAV2 and

Keywords

- capsid structure ■ gene therapy ■ parvoviruses
- pathogenicity ■ tissue tropism

MVM virions contain VP1, VP2 and VP3; and BPV1 contains VP1, VP2, VP3 and VP4. The amino acid sequences of the VPs are overlapping, with the entire sequence of VP3 (when present) contained within VP2, which is in turn contained within VP1. Sixty copies of these VPs, in a predicted ratio of 1:1:10 for VP1:VP2:VP3 (when present) or 1:10 for VP1:VP2, assemble the capsid with $T = 1$ icosahedral symmetry [11]. VP1, containing a unique N-terminal region (VP1u), is always the minor component in all virus capsids, while the smallest VP is always the major component.

The capsid, with its packaged ssDNA genome, has to traverse two cellular barriers during infection, the plasma and nuclear membranes, for replication in the cell nucleus (FIGURE 1). Like most other viruses, attachment to a cell surface receptor is an essential first step of parvovirus infection [12–14]. Extensive biochemical and molecular characterizations have led to the proposal that, following initial attachment, the parvovirus capsid is internalized through clathrin-coated pits [15,16] and trafficked through the endocytic pathway to the nucleus for genome replication, followed by transcription of the genome and translation of the message for production of the Rep/NS and VP required for the formation of progeny virus. Endosomal acidification is essential for the infection of all parvoviruses, with lysosomotropic drugs such as baflomycin A1 and chloroquine, which interfere with endosomal pH, blocking infection [12,13,16–21]. For the dependoviruses, there is evidence that some AAV serotypes are trafficked through the Golgi and endoplasmic reticulum en route to the nucleus, and for both dependovirus and autonomous members, cellular components, such as actin and dynein as well as microtubules [22–27], are proposed to be involved in cellular trafficking (FIGURE 1).

The parvovirus VP is capable of performing a wide variety of structural and biological functions during the viral life cycle, including host cell surface receptor recognition, intracellular trafficking, nuclear entry, capsid self-assembly, genome encapsulation, maturation to produce infectious virus progeny, nuclear exit and host immune response detection and evasion (reviewed in [28,29]). The relatively small parvoviral genome has allowed the use of genetic manipulation to identify functional domains/regions of the VPs/capsid. These studies show that the parvoviruses have evolved to utilize the VP1u for a phospholipase A₂ (PLA₂) function required for endosomal escape [30] and nuclear entry during infection [31–34], regions of VP2

for nuclear entry (in dependoviruses) and for nuclear exit (in some autonomous viruses), and amino acid stretches within the common VP1/2/3 region for receptor attachment, tropism and host range determination, capsid assembly, DNA packaging and host antibody recognition [28]. The role of capsid structure in facilitating these VP functions for dependoviruses and autonomous parvoviruses will be discussed below following an introduction to their capsid structure.

Towards correlating the capsid structure with its various functions during cellular infection, the 3D structures for several *Parvovirinae* members have been determined using x-ray crystallography and/or cryoelectron microscopy and image reconstruction (cryoreconstruction) [11,28,35–54]. In all these structures, only approximately 520 residues of the common C-terminal VP1/VP2 or VP1/2/3 region (depending on virus) are resolved, leaving the N-terminal extensions of the larger VP(s), which are proposed to be positioned inside the assembled capsid, unobserved, except for B19V [11,28,35–54]. Low copy numbers of the minor capsid proteins or differential conformations adopted by the N-termini, which are inconsistent with the 60-fold icosahedral averaging applied during structural determination, could result in the lack of N-terminal VP ordering. Cryoreconstruction studies of AAV capsids in which medium-resolution structures for capsids assembled with/without VP1 in addition to those containing only VP3 suggest that the VP1u is located in the interior of the capsid, underneath the icosahedral twofold axis [39,46,55]. For B19V, cryoelectron microscopy reconstruction of wild-type virions and empty particles showed VP2 N-termini exposed on the capsid surface [52,53].

The VP structure (the ordered ~520 residues) is highly conserved, even for members that are only approximately 20% identical at the amino acid sequence level, such as AAV2 and B19V [52]. The core consists of a conserved eight-stranded (β B to β I, named from N- to the C-terminus) antiparallel β -barrel motif and an α -helix (α A) (FIGURE 2A). An additional β -strand, β A, involved in antiparallel interactions with β B, is also present in all the *Parvovirinae* structures (FIGURE 2A). The remaining VP structure consists of loops inserted between the β -strands that contribute to the capsid surface topology. These loops also contain small stretches of β -strand structure (not shown in FIGURE 2A). The loops are named after the strands between which they are inserted, for example, the DE loop is inserted between

why we
dont see
N term in
the
structures

B19 N
term

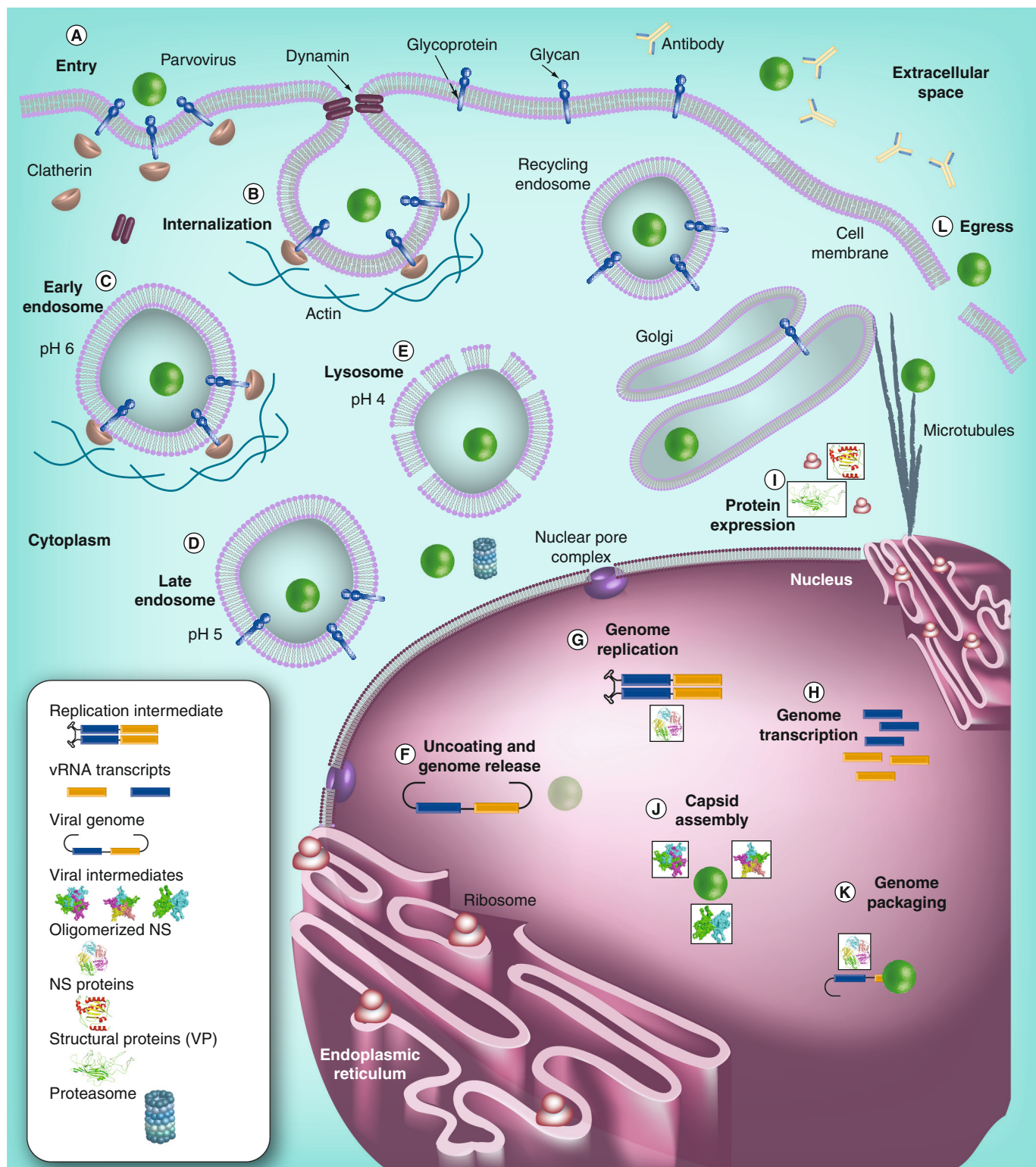


Figure 1. A schematic of the lytic infection life cycle of parvoviruses. (A) Primary receptor recognition. (B) Receptor-mediated endocytosis in clathrin-coated pits. (C–E) Trafficking through the endocytic pathway. (F) Capsid uncoating and genome release following nuclear translocation. (G) Genome replication. (H) Genome transcription. (I) Protein expression. (J) Capsid assembly following protein expression and translocation into the nucleus. (K) ssDNA genome packaging into empty capsids. (L) Newly formed virions exit the cell by nuclear exit for another round of infection. Steps that differ between members (e.g., proteasome targeting, Golgi and endoplasmic reticulum trafficking) are not labeled, and those that are poorly understood (e.g., nuclear translocation and nuclear exit) are not shown. The legend depicts the molecules associated with the life cycle.
NS: Nonstructural; VP: Viral protein.

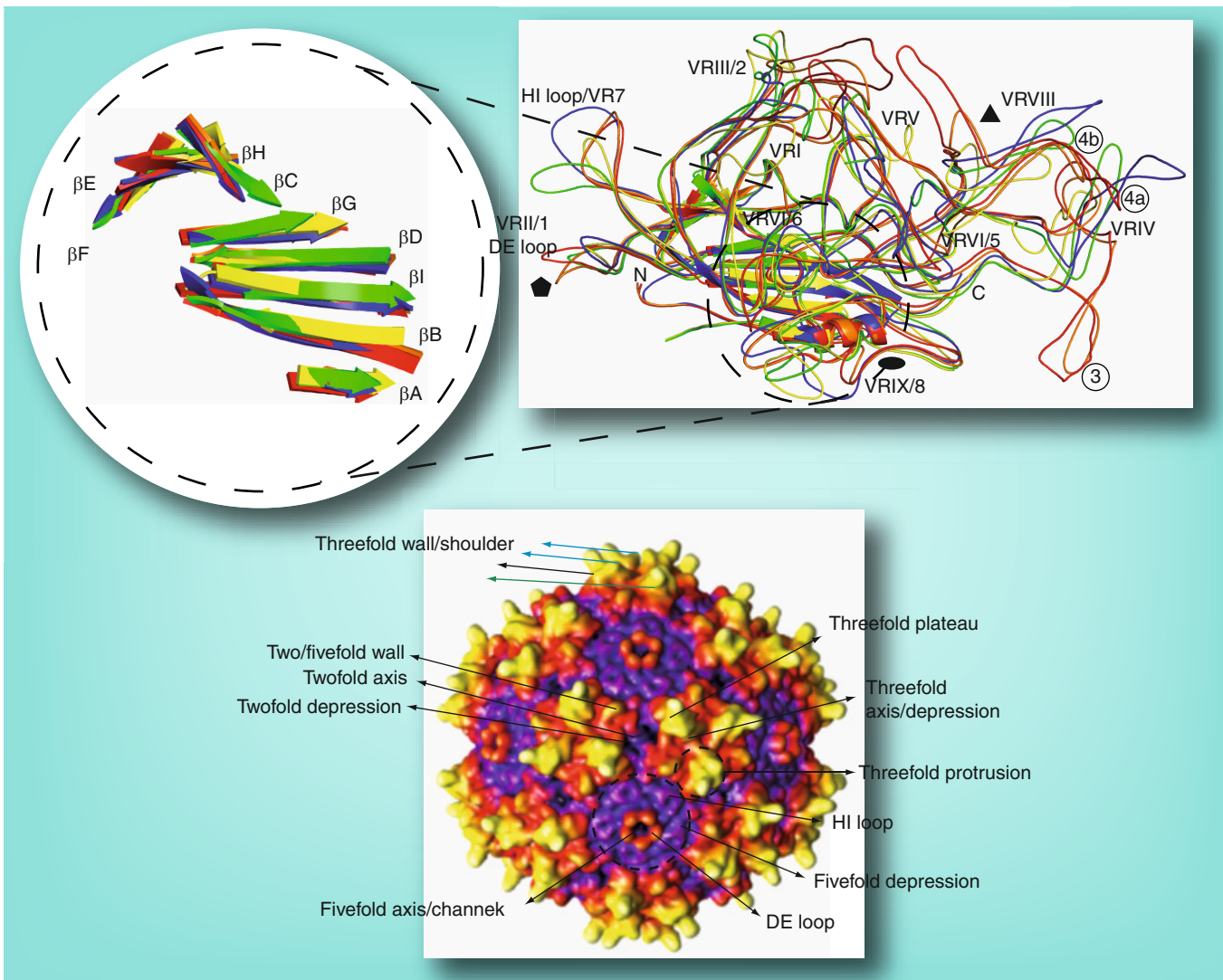


Figure 2. The parvovirus capsid viral protein and adeno-associated virus serotype 2 capsid structure. (A) Conserved secondary structure superposition of the structurally ordered viral protein region for type members of the *Parvovirinae* subfamily, with the exception of *Bocavirus* (for which the structure of human bocavirus 1 [HBoV1] is shown): *Amdovirus* – Aleutian mink disease virus (red); *Bocavirus* – HBoV (yellow); *Dependovirus* – adeno-associated virus serotype 2 (AAV2; blue); *Erythrovirus* – human parvovirus B19V (green); and *Parvovirus* – minute virus of mice (orange). Atomic coordinates for AAV2, the prototype strain of minute virus of mice and human parvovirus B19V were obtained from the Research Collaboratory for Structural Bioinformatics (RCSB) protein database (PDB ID numbers 1lp3, 1z14 and 1s58, respectively). The Aleutian mink disease virus and HBoV1 images were generated from pseudo-atomic coordinates built into cryoreconstructions [48,51]. The approximate positions of icosahedral two-, three- and five-fold axes of symmetry of the capsid are depicted by the filled oval, triangle and pentagon, respectively. The N-terminus, C-terminus, variable regions (VRI–IX, VR1–8) and DE and HI loops are labeled. The encircled region shown in the top left depicts just the β A and β -barrel motif (β BIDG- β CHEF) conserved in all parvovirus viral protein structures determined to date. (B) Surface representation of AAV2 used to illustrate the topological features of the parvovirus capsid surface as discussed in the text. The different colored arrows for the 'threefold wall/shoulder' label indicate the wall of the threefold protrusion facing the icosahedral twofold axis (black), icosahedral threefold axis (blue) and fivefold axis (green). The image is depth-cued (blue–red–yellow–white) to show regions at the shortest radial distance to capsid center in blue and those at the furthest radial distance in white (see Figure 3 for radial distances). (A) was generated using the PyMol program [243] and (B) was generated using the UCSF Chimera program [244]. (B) is reproduced with permission from [51].

β -strands β D and β E and the HI loop is inserted between β H and β I. The tops of these loops are structurally varied between members in the same and different genera, and dictate host-specific tropism, antigenic response and transduction efficiency in viral vectors. The BIDG β -sheet forms the interior surface of the capsid, while

the inserted loops form characteristic features at and around the icosahedral two-, three- and five-fold axes of symmetry (Figures 2B & 3). There is a depression at each twofold axis; a single protrusion at the threefold axis of members of the *Parvovirus* genus (e.g., MVM, *Canine parvovirus* [CPV], *Feline panleukopenia virus*

[FPV], *Porcine parvovirus* [PPV]) or three separate protrusions surrounding the ‘depression’ at the threecold axis (FIGURE 2B) in members of the *Amdovirus* (e.g., ADV), *Bocavirus* (human bocavirus [HBoV]), *Dependovirus* (AAVs) and *Erythrovirus* (B19V) genera; a cylindrical channel at each fivefold axis; a depression surrounding the cylindrical channel; and a ‘wall’ between the two- and five-fold depressions (FIGURES 2B & 3) [11,28]. The protrusions are more pronounced in ADV and the AAVs compared to B19V and HBoV1 (FIGURES 2B & 3). B19V and HBoV1 appear to share characteristics of members of the *Parvovirus* and *Dependovirus* genera and have flatter protrusions (FIGURE 3). The twofold axis (in all the virus structures) is created by the loop after β I from two twofold symmetry-related VP monomers; the single threecold protrusion in

members of the *Parvovirus* genus is created from six loops (within the GH loop), two from each threecold symmetry-related VP monomer; each of the three separate protrusions in the other *Parvovirinae* members are created by three loop regions (also within the GH loop) from two VP monomers; the fivefold channel is created by five symmetry-related DE loops and the surface of the depression surrounding this axis is lined by the HI loop (FIGURES 2 & 3).

the 3-fold protrusions for Parvo versus

Dependovirus: overview of AAVs

The AAVs were discovered in 1965, associated with Ad infections, hence their name [1,5,56,57]. Their classification as dependoviruses is based on their requirement for coinfection with helper viruses (e.g., Ad or HSV) to complete a lytic infection. In the absence of the helper viruses,

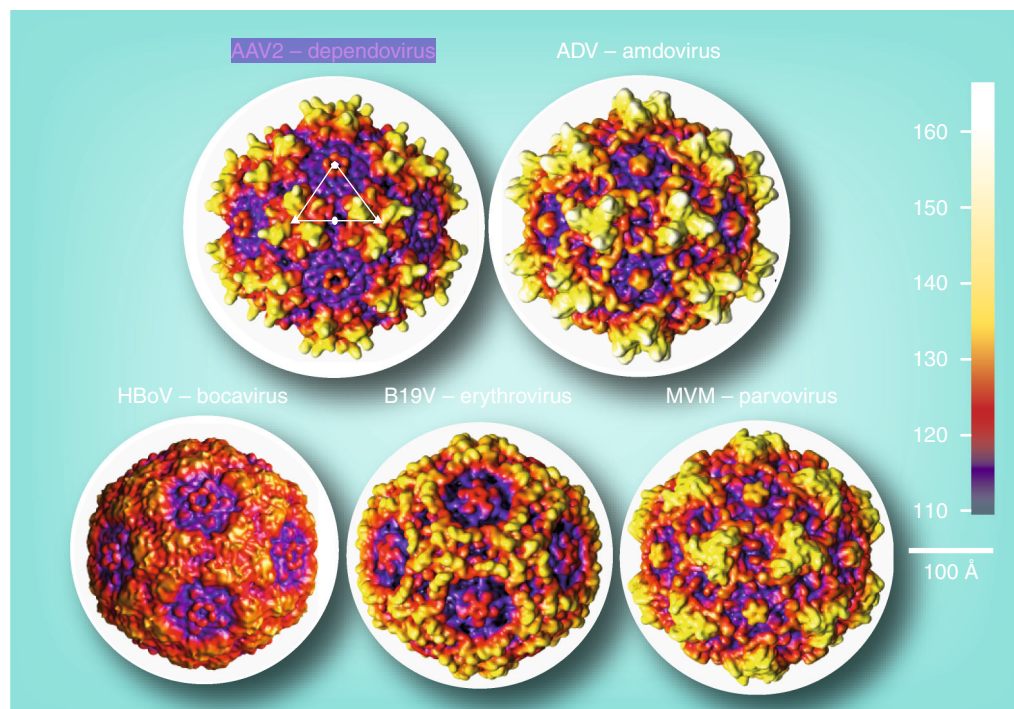


Figure 3. Capsid features of Parvovirinae subfamily members. Depth-cued (blue–red–yellow–white) capsid surface representation of type members of the five genera of *Parvovirinae* viruses, with the exception of *Bocavirus* (for which HBoV is shown instead of bovine parvovirus 1). Each virus and the genus to which it belongs are labeled. The virus images show topological features (illustrated in FIGURE 2B with AAV2) at and around the two-, three- and five-fold axes of symmetry of the capsid surface for each member. The more pronounced protrusions of AAV2 and ADV are white at their peak. A viral asymmetric unit (white triangle), bounded by a fivefold axis (filled pentagon) and two threefold axes (filled triangles) separated by a twofold axis (filled oval), is shown on the AAV2 image. Sixty of these make up the T = 1 icosahedral capsid. In the parvoviruses, symmetrical viral protein monomers make up the viral asymmetric unit. A horizontal scale bar (100 Å) for diameter measurement is shown on the right-hand side, and a vertical color bar for radial distance (Å) from the center of the particle is also shown on the right-hand side. These figures were generated using the UCSF Chimera program [244]. The coordinates used were obtained as described in the legend of FIGURE 2A.

AAV: Adeno-associated virus; ADV: Aleutian mink disease virus; B19V: Human parvovirus B19V; HBoV1: Human bocavirus 1; MVM: Minute virus of mice.
Reproduced with permission from [51].

dependoviruses undergo a latent infection that can be reactivated by the introduction of helper virus. These viruses are nonpathogenic and able to package foreign DNA, resulting in intense efforts to develop several members of this genus as vectors for therapeutic gene delivery applications. Currently clinical trials are underway with AAV vectors packaging therapeutic genes for the treatment of several diseases, including $\alpha 1$ -antitrypsin deficiency, Leber's congenital amaurosis, muscular dystrophy, hemophilia B, cystic fibrosis, Alzheimer's disease, arthritis, lipoprotein lipase deficiency, Parkinson's disease and HIV infection [58–63]. Challenges for these clinical studies include the need to improve viral–tissue specificity and decrease the detrimental effects of the host immune response against the vector (especially for treatments that may require vector readministration) [64,65]. Efforts to overcome these issues have included the isolation and characterization of novel AAV serotypes and/or variants to exploit their tissue tropisms, transgene expression efficiencies and, hopefully, lack of human immune system recognition. To date, 12 AAV serotypes (AAV1–12) and over 100 gene sequences have been isolated from human/non-human primate tissues [66]. Aminoacid sequence (VP1) comparison between the 12 serotypes shows approximately 60–99% identity, with AAV4 and AAV5 being the most different [66]. In addition, AAV sequences have been isolated from several hosts, including caprine, mouse, bovine, snake, lizard and avian tissues [67–71], which share different levels of sequence similarity with the isolates from the human and nonhuman primate sources.

While AAV2 is the most-studied and best-characterized serotype, *in vivo* studies have shown that other serotypes can exhibit higher transduction and/or expression efficiencies for specific tissues compared to AAV2. For example, AAV9 demonstrates the highest protein expression level distributed among different tissues, while AAV7 has a comparable expression level in liver cells [72]. In addition, higher levels ($\sim 10^3$ -fold) of protein expression were observed with AAV1 and AAV6 in the heart, lung and skeletal muscle compared to AAV2 [66,73–75]. Amino acid and structural differences are reported to dictate disparities in receptor recognition, transduction efficiency and antigenic recognition between the AAVs.

AAV capsid structure & capsid-cell surface receptor interactions

Currently, atomic structures of nine serotype members, AAV1–9, serving as the representative

members of the AAV antigenic clades and clonal isolates [66], have been determined using x-ray crystallography and/or cryoreconstruction [11,35–41,47] [GOVINDASAMY L ET AL., UNPUBLISHED DATA]. For these viruses the conserved core regions (β B– β I and α A) are superimposable while the tops of the loops between these conserved regions are varied in sequence and structure and are defined as variable regions (VRs) I–IX (FIGURE 2A) [49]. Mutagenic, biochemical and structural studies have demonstrated that residues in these VRs are crucial in the virus life cycle, including virus–receptor binding (reviewed in [29]).

Biochemical studies have identified primary receptors and coreceptors utilized for initial cellular recognition and internalization, respectively, during infection by the AAVs (TABLE 1) [76–97]. With respect to primary recognition, several glycans are utilized by the AAVs. Heparan sulfate (HS) proteoglycan serves as the cell surface receptor for AAV2 and AAV3b (closely related to AAV2), terminal N-acetyl neuraminic acid (sialic acid [SA]) for AAV1, AAV4, AAV5 and galactose for AAV9 (TABLE 1) [29,76–78,80–91,95,96]. AAV6 is able to utilize HS or SA depending on the cell type being infected (TABLE 1) [90,91]. The primary receptor for the other human and non-human primate AAV serotypes, AAV7, AAV8 and AAV10–12, are yet to be determined. Bovine AAV utilizes gangliosides for transduction and chitotriose, a trimer of β -1–4-linked N-acetyl glucosamine found on gp96, for cellular transcytosis [79,97]. The residues involved in glycan interactions have only been characterized for AAV2, AAV5 and AAV6 as discussed below.

Mutagenesis of AAV2 followed by structure determination of AAV2–HS complexes mapped VP residues involved in the AAV2–HS interaction to several structurally adjacent basic residues R484, R487, K532, R585 and R588 (AAV2, VP1 numbering) (FIGURE 4), consistent with the highly acidic nature of HS molecules [95,96,98,99]. These AAV2 residues are located at the inner wall of the protrusions surrounding the threefold axis (FIGURES 2B & 4). They are located in three VRs; VRV, VRVI and VRVIII. Residues in VRV from one AAV VP interacts with VRIV and VRVIII from another threefold symmetry-related VP to assemble the top of the protrusions surrounding the threefold axis, while VRVI forms the base of the protrusions facing the twofold axis [95,96]. Thus, the binding site is only present on assembled capsids. The structure of AAV2 complexed with a HS oligosaccharide [95,96] showed the location of the bound HS molecules adjacent

Table 1. Parvoviruses, their receptors and their hosts.

Virus	Receptors	Coreceptor	Host	Ref.
AAV1	α 2–3 and α 2–6 N-linked sialic acid	–	Human	[90]
AAV2	HSPG	Integrin $\alpha_5\beta_1$, $\alpha_v\beta_5$, FGFR1, HGFR, LamR	Human	[76,81,83,86,87,92]
AAV3	HSPG	HGFR, LamR, FGFR1	Human	[76,82,101]
AAV4	α 2–3 O-linked sialic acid	–	NHP	[93]
AAV5	α 2–3 and α 2–6 N-linked sialic acid	PDGFR	Human	[78,84,88,93]
AAV6	α 2–3 and α 2–6 N-linked sialic acid, HSPG	EGFR	Human	[89–91]
AAV8	–	LamR	NHP	[76]
AAV9	Galactose	LamR	Human	[76,77,85]
Bovine AAV	Gangliosides, chitotriose	–	Bovine	[79,97]
ADV	ADV-binding protein	–	Mink	[173]
BPV1	Sialic acid	Glycophorin A	Bovine	[94,174]
B19V	Erythrocyte P antigen	Integrin $\alpha_5\beta_1$, ku80	Human	[175–177]
MVM	Sialic acid	–	Rodent	[178–180]
CPV and FPV	Sialic acid	Transferrin receptor	Cat, dog	[19,182]
PPV	Sialic acid	–	Swine	[26]

AAV: Adeno-associated virus; ADV: Aleutian mink disease virus; B19V: Human parvovirus B19V; BPV: Bovine parvovirus; CPV: Canine parvovirus; FPV: Feline panleukopenia virus; HSPG: Heparan sulfate proteoglycan; MVM: Minute virus of mice; NHP: Nonhuman primate; PPV: Porcine parvovirus.

to the residues mapped by mutagenesis. Levy *et al.* also reported structural rearrangements of the HI loop on the canyon floor surrounding the fivefold channel, which they proposed could be related to the opening of the channel to prime the capsid for externalization of the VP1u for endosomal escape or genome release following nuclear entry [96].

The capsid amino acids involved in glycan recognition have been reported for AAV5 and AAV6. AAV5 utilizes α 2–3 N-linked SA for infection [88,93]. A single-residue mutation, A581T (AAV5, VP1 numbering), affects airway cellular transduction shown to require SA binding [100]. This residue, structurally equivalent to AAV2 A591 (FIGURE 4), is also located on the inner wall of the threefold protrusion in the AAV5 capsid structure [GOVINDASAMY L, AGBANDJE-MCKENNA M, UNPUBLISHED DATA]. AAV6 and the closely related AAV1 recognize α 2–3 and α 2–6 N-linked SA for cellular infection, with AAV6 also able to utilize HS as a cellular receptor [90,91]. Mutagenesis studies, in which the six amino acids (129, 418, 531, 584, 598, 642 and AAV1/6 VP1 numbering) that differ between the two viruses were reciprocally changed, identified K531 in AAV6 as playing an important role in

HS recognition, with a change to the E531 present in AAV1 abolishing this interaction [91]. This residue, structurally equivalent to E530 in AAV2 (FIGURE 4), is located on the AAV6 capsid surface at the base of the threefold protrusion within the vicinity of the AAV2 HS residues, but is on the wall facing the twofold depression rather than the threefold depression (FIGURE 2B) [36]. Recently, a second mutagenesis study identified another AAV1/6 residue, K459, as being important for AAV6 heparan sulfate proteoglycan recognition [35]. This residue is structurally equivalent to AAV2 S458 (FIGURE 4) located at the plateau close to the top of the threefold protrusion (FIGURE 2B) and is not adjacent to K531. The AAV2–HS mutagenesis and structure data combined with the mutagenesis data for AAV5 and AAV6 suggests that the AAVs commonly utilize amino acids in the threefold region for recognition of different carbohydrate moieties.

Following the recognition of a cell surface receptor by the AAVs, an interaction with cell membrane proteins, which serve as coreceptors, is required for capsid internalization (TABLE 1). For AAV2, several internalization coreceptors have been identified, including integrin $\alpha_v\beta_5$, integrin $\alpha_5\beta_1$, FGFR1, HGFR and 37/67 kDa

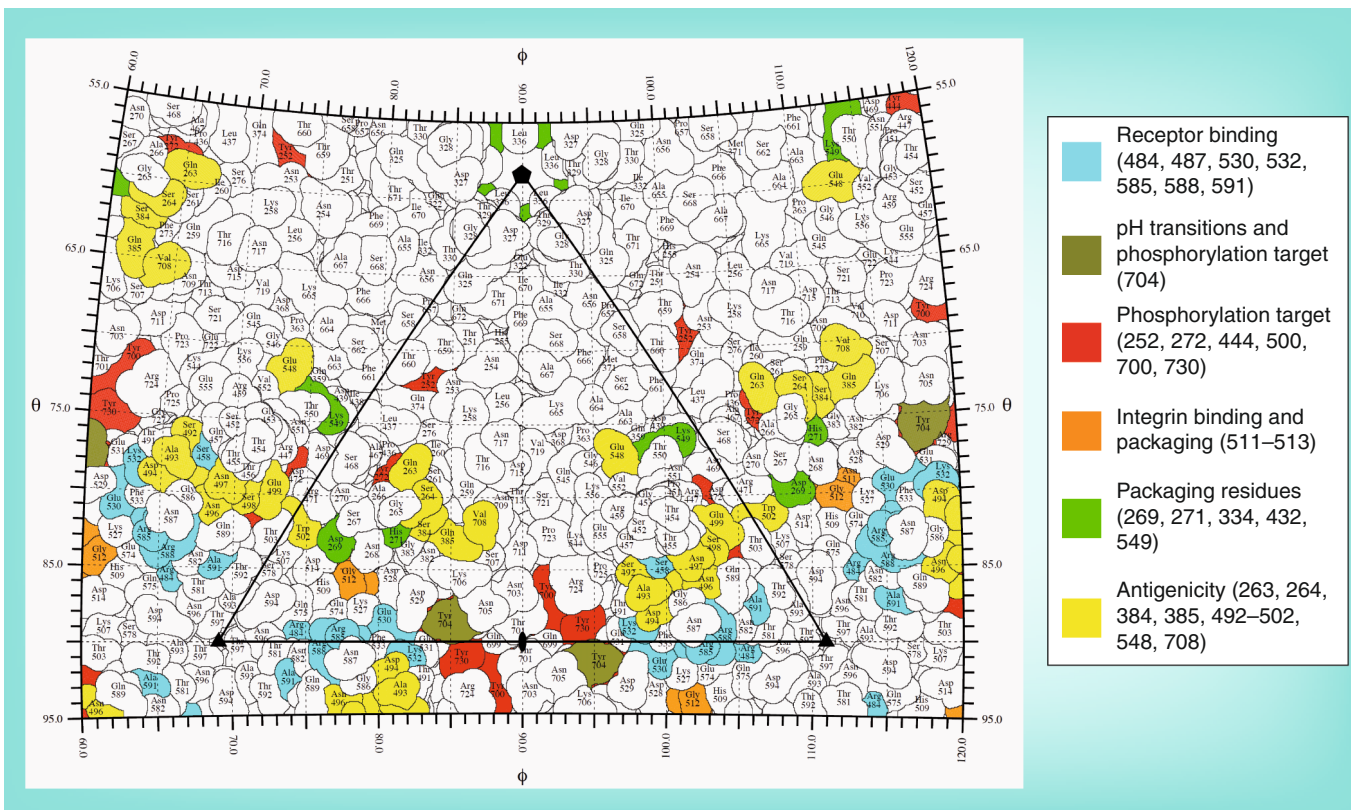


Figure 4. Stereographic roadmap projection of the surface residues of adeno-associated virus serotype 2. The black triangle delineates the residues in a viral asymmetric unit as described in **FIGURE 3**. Residues are labeled by type (three-letter code) and number (viral protein 1 numbering). The area occupied by each amino acid residue correlates to surface exposure when the capsid is viewed down the icosahedral twofold axis. The boundary for each residue is shown in black, and the residues important for receptor binding, pH transitions, capsid phosphorylation, integrin binding/genome packaging and antibody binding are filled in different colors as indicated in the color key shown on the right-hand side. In this image, symmetry-related residues are not distinguished. The adeno-associated virus serotype 2 coordinates were obtained as described in the legend of **FIGURE 2A**. Generated using the program RIVEM [245].

LamR [76,81,83,86,92]. LamR was actually identified as a coreceptor for AAV8 that could also serve a similar function for other AAVs, including AAV2, AAV3b and AAV9 [76], and, similar to AAV2, AAV3b also utilizes HGFR and FGFR1 as its coreceptors [76,82,101]. The interaction between AAV3 and HGFR appears to be specific for human cell-derived HGFR (hHGFR), while AAV2 is also able to bind the murine derived receptor, mHGFR. Sequence differences between the murine and human receptors are suggested as a source of the differential AAV3 and AAV2 recognition [82]. Other proteins required for internalization of other AAV serotypes include PDGFR and EGFR for AAV5 and AAV6, respectively [78,89]. For the AAV coreceptors, the VP residues important for $\alpha_5\beta_1$ and LamR binding have been identified [76,92], but the binding sites for the other coreceptors are unknown. A 511–NGR–513 motif (AAV2, VP1 numbering), was reported to play a role in binding to $\alpha_5\beta_1$ [92]. These residues are located close to the base of the threefold protrusion

(two-/five-fold wall; **FIGURE 2B**), proximal to the HS binding residues with G512 exposed on the capsid surface (**FIGURE 4**). The NGR sequence is conserved in most of the AAV serotypes, with the exception of AAV4, AAV5 and AAV11. This motif is partially conserved in B19V, which utilizes $\alpha_5\beta_1$ as a receptor (see below). Due to the close proximity of this region to the HS binding site in AAV2, it has been postulated that the primary HS receptor binding might promote this AAV2 capsid–coreceptor interaction, or serve as a prerequisite. The binding site for LamR on the AAV8 capsid was mapped to two large peptide regions containing residues 491–547 and 593–623 (AAV8, VP1 numbering) [76]. These residues are located on the inner surface of the AAV8 threefold protrusions facing the threefold axis [38] and include GH loop amino acids in VRV and VRVI in the first stretch of amino acids and residues in a structurally conserved VP region past VRVIII and before the β H strand in the second stretch. The report that this receptor is utilized by several AAVs would thus suggest

that second stretch of residues, 593–623, conserved in sequence and structure [38], may be more important for this recognition. These residues, structurally equivalent to residues 590–620 in AAV2 (FIGURE 4), are close to those reported to bind HS in AAV2 and SA in AAV5, with surface amino acids clustered around the three-fold axis (FIGURE 4). The proximity of the LamR footprint to AAV primary glycan recognition regions, as for the $\alpha_5\beta_1$ motif, again suggests the possibility that the initial cell surface recognition leads to a subsequent engagement of LamR for internalization.

AAV capsid internalization & trafficking

The interaction of the AAV capsid with internalization receptors results in host cell surface rearrangement, which is a prerequisite for endocytosis, a clathrin-mediated process [102]. Several immunofluorescence microscopy and chemical inhibition studies showed AAV capsids colocalized with dynamin and microtubules as well as markers from early, late and recycling endosomes, and lysosomes (FIGURE 1) (reviewed in [22]). In addition, endosomal processing is reported to be the rate-limiting step in viral transduction in several cell lines [29,103]. Biochemical experiments confirmed that the AAV VP1u (amino acids 1–137, VP1 numbering) is exposed during endosomal trafficking [104,105]. Once exposed, the VP1u PLA₂ activity hydrolyzes membrane phospholipids to cause the endosomal membrane rearrangement required to facilitate viral capsid release [30]. During the transition from early to late endosomes, acidification-induced capsid structural changes, including the externalization of the VP1u, are reported to be essential for viral trafficking, uncoating and genome release in nucleus. However, pH alone is not sufficient to mediate VP1u externalization for the AAVs, suggesting a requirement for yet-to-be-identified cellular factors in this capsid transition [46]. Artificial heat treatment (65°C) alone can mimic the endosomal conditions required for VP1u externalization in the presence of viral genome [46]. Higher temperatures (75°C) are required to release the VP1u in capsids that are devoid of DNA [46]. As discussed above, the structure of VP1u inside the capsid or in its externalized state has not been structurally observed, but is predicted to be α -helical in nature, as reported for other PLA₂ domains. Mutagenesis and biochemical studies suggest that the fivefold channel (FIGURE 2B) might play a role in its extrusion [105]. Confocal microscopy studies have shown that, in addition to the trafficking through

the endocytic pathway, AAV2 can localize to the secretory pathway en route to the nucleus [27], while electron and immunofluorescence microscopy have observed AAV5 in the Golgi compartment (FIGURE 1) [25,106]. Further studies are required to characterize the role of these alternative trafficking routes and the role of capsid interactions in facilitating them.

The AAV8 capsid structure is the best characterized serotype with respect to the effect of the pHs encountered in the endocytic pathway. Structures determined by x-ray crystallography to 2.7-Å resolution for capsids incubated at pH 7.5, pH 6.0, pH 5.5 and pH 4.0 identified two regions affected by pH that are conserved among the AAVs [107]. The first region, designated as the ‘pH quartet’, involves residues R392, H529, E566 and Y707 (AAV8, VP1 numbering), and is located close to the icosahedral twofold axis, with residue Y707 (equivalent to AAV2 Y704 in FIGURE 4) visible on the capsid surface. The amino acid side-chain transitions occurring as pH decreases result in a reduction in the number of interactions between twofold-related VP monomers and ‘weaken’ this interface [107]. It was thus proposed that amino acids at the twofold interface may be involved in capsid destabilization events that enable AAV VP1u externalization without capsid disassembly. The second region is located on the capsid interior surface under the threefold axis and involves residues F631 and H632 (AAV8 VP1 numbering). Previous structural studies have assigned this region as the nucleic acid binding pocket for AAVs [36–38,49] and implied a role in AAV genome stabilization.

A low pH-induced H632 side-chain conformational change disrupts the interaction of the VP with the ordered nucleic acid density observed in crystal structures. The loss of this density was suggested to prime the capsid for genomic uncoating. Thus, similar to other viruses [108,109], this study suggests that the AAV viral genome undergoes rearrangement inside the capsid prior to its release and that altered capsid–genome interactions, triggered by pH, are important aspects of cytoplasmic preprocessing prior to nuclear entry for genomic uncoating.

Several cellular host protein machineries have been reported to interact with the AAV capsid during trafficking to the nucleus that are detrimental to infection. As an example, the targeting of AAV2 capsids to the proteasome in the cytoplasm is reported to limit viral transduction efficiency [110,111]. Phosphorylation of capsid surface-exposed tyrosines followed by ubiquitination is reported to be the signal for recognition

nucleotide
binding site and
capsid
disassembly

2-fold imp for transduction

by the proteasome and subsequent capsid degradation. Mutation of the seven AAV2 capsid surface-exposed tyrosine residues, Y252, Y272, Y444, Y500, Y700, Y704 and Y730 (AAV2 VP1 numbering) to phenylalanine resulted in a significant (up to ~700-fold) increase in transduction efficiency dependent on cell line [111]. Significantly, AAV8 Y707, equivalent to AAV2 Y704, clustered at the icosahedral twofold axis with Y700 and Y730, undergoes the pH-mediated transition discussed above, consistent with a role in capsid–cellular interactions during trafficking.

The exact mechanism of AAV genome translocation into the host cell nucleus following escape from cytoplasmic compartments is poorly understood, as are the determinants of capsid uncoating in the nucleus. The VP1/VP2 N-terminal regions contain nuclear localization signals (NLSs) that, when mutated, significantly reduce AAV infectivity [31–34]. These N-terminal VP regions can be detected by antibodies in the cytoplasm of infected cells, indicating that they become externalized prior to nuclear entry [31]. Capsid processing prior to cytoplasmic release and subsequent nuclear entry, as suggested by the pH-mediated structural changes described above and the reported release of the VP1u N-terminus, is consistent with the observation that microinjection of virions into the cytoplasm does not confer a nuclear translocation phenotype, even if the N-terminal regions are pre-exposed by heating [31]. While the size of the AAV capsid at approximately 260 Å in diameter is small enough to be translocated through the nuclear pore complex, there are conflicting reports on the issue. Some reports say that it can, while others say that this may not be the case [112,113]. The exact mechanism remains to be elucidated.

AAV capsid uncoating, genome replication, capsid assembly & genome packaging

The majority of studies indicate that AAV genome uncoating occurs in the nucleus [12,31,34,112,114,115]. However, there are reports that uncoating may occur before or during nuclear entry [116]. Regardless of the uncoating site, the capsid transitions resulting in genome release following nuclear entry remain poorly understood and likely requires cytoplasmic pre-processing, some discussed above, prior to nuclear entry [34].

Following viral genome release into the nucleus, rolling hairpin replication is proposed

as the mechanism for parvovirus genome replication [117]. However, little is known about the role of the capsid protein in this process. Two elements of the AAV genome shown to be indispensable for replication are the inverted terminal repeats and the p5 *rep* transcript. The two large replication proteins, Rep78 and 68 (Rep78/68), encoded by the *rep* ORF and translated from the p5 transcript, possess terminal resolution site endonuclease, DNA terminal repeat binding, and DNA 3'-5' helicase activities. Viruses with mutations in the Rep78 and Rep68 nucleotide binding regions are defective for viral DNA replication [118–120]. *In vitro* studies show that after successful genome replication, the viral ssDNA genome is packaged into preassembled empty capsids in the nucleus [121–123].

Expression of the AAV VPs alone is sufficient for capsid assembly, suggesting that genome packaging is not required for this process [124]. However, density consistent with a nucleotide is observed in most of the AAV capsid structures determined to date, including virus-like particles expressed in heterologous systems in the absence of viral genome. This suggests a requirement for VP–DNA interaction in capsid assembly. Recent studies identified a transiently expressed 23kDa protein, AAP, which is required for capsid assembly [55,125]. This protein, expressed from a newly identified ‘ORF2’ of the *cap* gene, targets VPs into the nucleolus, where capsid assembly is proposed to occur. Interestingly, comparison of capsid assembly for AAV1, 2 and 5 showed that AAV5 requires its own AAP and cannot be complemented by the AAV2 AAP. AAV5 is one of the most sequence-diverse serotypes of AAV1–12 [66], and this observation suggests that AAP engages in specific interactions with the VP during assembly. The step in capsid assembly requiring AAP is yet to be determined. Site-directed mutagenesis studies have identified several AAV VP residues that are important for capsid assembly. These are mostly charged residues involved in symmetry interface interactions (reviewed in [29]). Significantly, residues in the HI loop, which forms the majority of the fivefold symmetry-related interactions in assembled AAV capsids (FIGURE 2), play a role in capsid assembly as well as genome packaging [33,126].

The AAVs package both strands of their ssDNA genome with equal frequency into different capsids in a process that is highly dependent on the small replication proteins, Rep52 and Rep40, which are encoded by the *rep* ORF. A reduction in expression of these proteins results in a significant decrease in packaging efficiency

[127]. Biochemical studies have shown that oligomeric Rep 52/40 has a 3' to 5' helicase activity [128], which is believed to interact with the assembled empty capsid and unwind the replicative products of AAV genome for packaging into the capsid. The interactions between Rep 52/40 and the AAV capsid have been reported to be both DNA-dependent and -independent [129–134].

Regions of the Rep responsible for virus–capsid interaction and/or DNA binding have been identified within residues 322–482 (Rep78 numbering). However, the capsid portal required for AAV genome packaging remains unclear. Mutagenesis of AAV2 capsid residues surrounding the fivefold channel resulted in significant reduction (~3–9 times) in genome packaging (especially D219, V221, N334 and S338, VP1 number) (FIGURE 4) [32,105]. These AAV2 residues are located at the base of the fivefold channel (219 and 221) or in the DE loop (334 and 338) forming the channel (FIGURE 4). In addition, a single amino acid change, R432A, in AAV2, which is partially buried within the capsid shell under the threefold protrusions, is normal for capsid assembly but significantly defective in genome packaging [32]. The AAV2 crystal structure shows the side-chain amino groups of R432 extending towards the capsid surface to interact with the main-chain carbonyl groups of residues D269 and H271 in a threefold symmetry-related VP, located on the capsid surface on the two-/five-fold wall (FIGURES 2B & 4). A mutation to alanine would disrupt this interaction and perturb potential stabilizing interactions or alter the capsid surface topology. Unlike wild-type AAV2, the capsid of the R432A mutant has a permanently externalized VP1 N-terminus detectable by the A1 VP1u monoclonal antibody without heat treatment, and it has an increased affinity for Rep proteins [124]. Other amino acids that, when mutated, affect genome packaging include the 511–NGR–513 motif mutated to RGD, and mutations at residues 520, 540 and 549 (reviewed in [29]). These amino acids are not adjacent and are located on the wall between the two-/five-fold wall (269, 271 and 512) or the threefold protrusion, with 520 and 540 buried inside the protrusions and 549 on the surface of the protrusions facing the fivefold axis (FIGURES 2B & 4). Interestingly, the VP loop containing 511–513 is immediately adjacent to the VP loop containing residues D269 and H271 (FIGURE 4) and the side-chain of R432A (not surface-exposed) from a threefold symmetry-related VP. Collectively, the available data implicate the fivefold channel and DE loop in DNA packaging, and the capsid

surface close to or on the protrusions in direct or indirect Rep binding.

Post-capsid assembly and genome packaging, wild-type AAV virions must exit the nucleus and traffic to the cell surface for a second round of infection. However, very little is known about this process or the role of the capsid in facilitating it for the dependoviruses.

AAV capsid-mediated antigenic response

Host immune system response is an important line of defense against infecting pathogenic viruses. However, while the AAVs are not pathogenic, given their development as gene therapy vectors, it is important to understand their capsid antigenic properties. Information arising from these studies is important for developing vectors that can avoid a pre-existing immune response either during the first administration or subsequent readministration of a therapeutic gene, while maintaining an efficient transduction phenotype. Both T-cell- and B-cell-mediated immune responses directed against the AAV capsid during vector delivery have been reported [135–138], with pre-existing host immune responses shown to be a major obstacle to gene delivery [139,140].

The AAV2 capsid is the most antigenically characterized using antibodies generated from mice, including two neutralizing antibodies, A20 and C37-B [141]. Peptide scanning and site-directed mutagenesis mapped the A20 epitope to residues 263, 264, 384, 385, 548 and 708 [141,142]. These residues are clustered on the two-/five-fold wall (FIGURES 2B & 4) and include amino acids in VP VRI, VR III, VR VII and VR IX. The A20 antibody blocks infection at a post-attached step that is not yet determined. The C37-B antibody recognizes AAV2 residues 492–502 and 602–610 [140]. Residues 492–502 are located in VP VRV and are exposed on the capsid surface on the top of the protrusions (plateau) surrounding the threefold axis (FIGURES 2B & 4) and are likely the major antibody contact region. Residues 602–610 are close to VR VIII and are buried close to the threefold axis and likely play a minor role in capsid recognition. These epitopes are proximal to the AAV2 HS binding site (FIGURE 4), which explains the blocking of AAV2 receptor recognition by C37-B binding [141]. In a study screening pooled human sera and intravenous immunoglobulin against a large panel of AAV2 capsid surface mutants, residues in VRI and IV–IX were observed to play a role in antibody recognition. These capsid regions

block of receptor binding site by antibody

also overlapped with binding site for the HS, were close to a proposed $\alpha_5\beta_1$ coreceptor binding site and contained surface amino acids shown to determine cellular transduction efficiency [142]. Thus, host neutralization could involve a myriad of inhibited interactions.

Several mouse monoclonal antibodies are available for a number of other AAV serotypes [143,144], creating reagents for characterization of the AAV infectious life cycle as well as defining steps at which neutralization can occur. The next challenge in defining the antigenic structure of the AAVs will be to structurally characterize the precise binding sites for neutralizing antibodies on the capsid of several serotypes being developed for delivery applications, and to determine whether a common epitope exists among the serotypes. It will also be important to visualize the spatial relationship between these epitopes and the capsid regions that are utilized for receptor recognition, determinants of transduction efficiency and other steps in the infection process. Information on a common AAV capsid epitope combined with information on cellular interaction sites will enable the recombinant DNA engineering of a vector ‘pill box’ with minor antigenic site modifications so that each vector will be antigenically novel when delivered. Ideally, these vectors would retain their natural host tropism while being able to circumvent the pre-existing immune response and avoid neutralization.

Autonomous parvoviruses: overview of genera type members

The autonomous parvoviruses encompass the members of four different *Parvovirinae* genera: *Amdovirus*, *Bocavirus*, *Erythrovirus* and *Parvovirus*. These viruses require cellular proliferation factors expressed transiently during the S phase for their DNA replication, but cannot induce resting cells to enter S phase (reviewed in [145]). Productive replication only occurs in rapidly dividing cells, thus lethal infections typically occur in fetal or neonatal hosts or cell lineages that remain actively dividing even in adult life. The pathogenic members of the autonomous genera are associated with serious illness in the young of the species that they infect and in immunocompromised adults, while non-pathogenic members establish asymptomatic but persistent infections (reviewed in [146]). Within this group, some members exhibit a narrow host range, while others infect a wide variety of species or tissues. This pattern of host range, which is capsid-controlled, may be mediated at any step of the viral life cycle.

ADV, the type and only member of the *Amdovirus*, causes a persistent infection in adult mink associated with high levels of anti-viral antibodies, plasmacytosis, immune dysfunction and progressive renal disease, and in newborn minks it causes a fatal, acute interstitial pneumonitis [147,148]. However, in spite of the elevated immune response, the virus is not neutralized *in vivo*, but instead circulates as virus–antibody complexes and leads to accelerated disease, because antibody binding enhances infection in macrophages via binding to Fc γ RII receptors [148,149]. This mechanism is termed antibody-dependent enhancement of infection (ADE) and has also been reported for dengue virus [150] and for B19V [151]. The highly pathogenic ADV-Utah 1 strain replicates poorly in cell culture, whereas the nonpathogenic ADV-G strain replicates permissively in Crandell feline kidney (CrFK) cells.

Members of the newly established *Bocavirus* genus include BPV1, *Canine minute virus* and the related HBoV1–4. These viruses share approximately 42–43% sequence identity in their capsid sequence, while the HBoV viruses are approximately 80–90% identical. The clinical symptoms of BPV1 infection include diarrhea and respiratory distress in neonatal calves, abortion and leukopenia [152]. The first HBoV virus, HBoV1, discovered in 2005 and classified in the *Bocavirus* genus, has been suggested to be the etiologic agent of respiratory tract infections and gastroenteric disease in children [153–158]. The newer isolates (HBoV2–4) were discovered mostly in stool samples but only HBoV2 has been associated with gastrointestinal ailments [159].

B19V, the type member of the *Erythrovirus* genus, infects humans and is associated with a wide variety of clinical manifestations, of which the most common is erythema infectiosum (or fifth disease) in children. Other serious symptoms include acute or persistent arthropathies, transient aplastic crisis in patients with underlying anemia (e.g., sickle cell anemia or thalassemia) and chronic anemia in immunocompromised patients; infection in pregnant women can result in hydrops fetalis and fetal myocarditis [160–164]. Other members of this genus infect nonhuman primates, such as rhesus and pig-tailed macaque parvoviruses and simian parvovirus [165].

The *Parvovirus* genus includes viruses that infect many different species, including mice, cats, dogs and pigs, and share medium (~50%) to very high (~98%) sequence identity. MVM, the type member for this genus, has two well-characterized strains that have served as a model

for probing the parvovirus capsid determinant of host range and pathogenicity. The immunosuppressive strain, MVMi, is pathogenic and causes acute leukopenia in immunocompromised mice [166], while the prototype strain, MVMp, is nonpathogenic and results in an asymptomatic infection [167]. MVMp was originally isolated from murine Ad stock and replicates efficiently in mouse fibroblasts, whereas MVMi, which was recovered from an EL-4 T-cell lymphoma, replicates in mouse T lymphocytes and hematopoietic precursors [168]. This and other rodent parvoviruses, including H1-PV and LuIII, display oncopreferential cytotoxic activity *in vitro* and oncosuppressive activity *in vivo* [169,170], and are being developed for cytoreductive and immunogene therapy approaches to target tumor cells [171].

Autonomous parvovirus capsid structure & capsid-cell surface receptor interactions

The capsid structure of at least one member of each autonomous parvovirus has been determined. The VP2 structures of all the autonomous members are superimposable, especially for the conserved β -barrel core and the α -helix (FIGURE 2A). However, as discussed above for the AAVs, there are certain surface loop regions that are structurally variable and have been defined as variable regions VR1–8 in the paper by Kontou *et al.* [172]. These loop differences, some of which overlap with those defined for the AAVs (FIGURE 2A), cluster around the fivefold axis, the threefold protrusions and depression at the twofold axis to create the characteristic surface features exhibited by the members of each different genus (FIGURE 3). As discussed above for the AAVs, the autonomous parvovirus VRs play important roles in the virus life cycle, such as receptor recognition, antigenic response and tissue tropism, and pathogenic outcome of infection.

Recognition of cell surface receptors by autonomous parvoviruses is a key parameter of tropism and pathogenesis. They use a wide variety of molecules, including carbohydrates, proteins and glycolipids, as receptors or coreceptors (TABLE 1). However, unlike the dependent viruses, there is no clear definition of which receptors serve as primary receptors for initial cell recognition and which are coreceptors used for internalization, except for B19V. For ADV, in addition to the antibody-mediated infection of macrophages via binding of the antibodies to Fc γ RII [148], an unknown 67-kDa protein, ABP, serves as a cellular receptor for entry into CrFK

cells [173]. BPV1 binds to sialylated membrane glycoproteins and especially glycoporphin A via O-linked α 2,3-linked SA [94,174]. B19V binds to the glycolipid erythrocyte P antigen (globoside) on erythroid progenitor cells, but requires $\alpha_5\beta_1$ integrins as coreceptors for cellular entry [175,176]. Ku80 has also been identified as a coreceptor for B19V infection [177]. For the *Parvovirus* genus, receptor information is available for MVM, CPV, FPV and PPV. MVM utilizes an SA-containing glycoprotein as a receptor [178] and has been shown to specifically bind α 2,3 linked sialylated glycans, including the s(Le^x)₃ glycan that contains the lewis X motif that is overexpressed in cancer cells, thus explaining MVM's oncotropism [179,180]. While both MVMp and MVMi bind the α 2,3 linked glycans, MVMi shows additional recognition to α 2,8 linked glycans that are overexpressed in neuronal cells, which likely mediate its neurotropism [180,181]. CPV and FPV use SA as an attachment factor during hemagglutination and their respective transferrin receptor (TfR) on canine and feline cells for infection [19,182]. The SA-CPV and SA-FPV interactions are not essential for infection [183]. Interestingly, FPV infects cats but not dogs as it is capable of using the TfR on feline cells, but is unable to bind the canine TfR. PPV also binds to SAs on cell surface glycoproteins [26].

The capsid region utilized for receptor recognition, tissue tropism or pathogenicity determination has been identified for several autonomous parvoviruses using biochemical, molecular and structural approaches. The discussion will focus on information available for the type members of the four autonomous parvoviruses genera. The difference in cell tropism of the ADV strains has been mapped to VP2 residues 92, 94, 115, 234, 238, 240, 241, 242, 352, 395, 434, 491 and 534, which cluster on or near the threefold protrusions and wall of the twofold depression of the pseudo-atomic model built into a cryoreconstructed density map (FIGURE 5) [48,184,185]. ADV residue 94 is structurally equivalent to CPV residue 93 involved in TfR receptor attachment as well as CPV/FPV host range and pathogenicity determination [186–188]. As with ADV residue 94, CPV residue 93 is located on CPV threefold protrusion, thus highlighting the utilization of common autonomous capsid regions for similar functions, as observed for the AAVs. Structural studies utilizing cryoreconstruction mapped the globoside receptor attachment site for B19V to the depression at the threefold axis [189], though recent studies [190] suggested that B19V did not bind

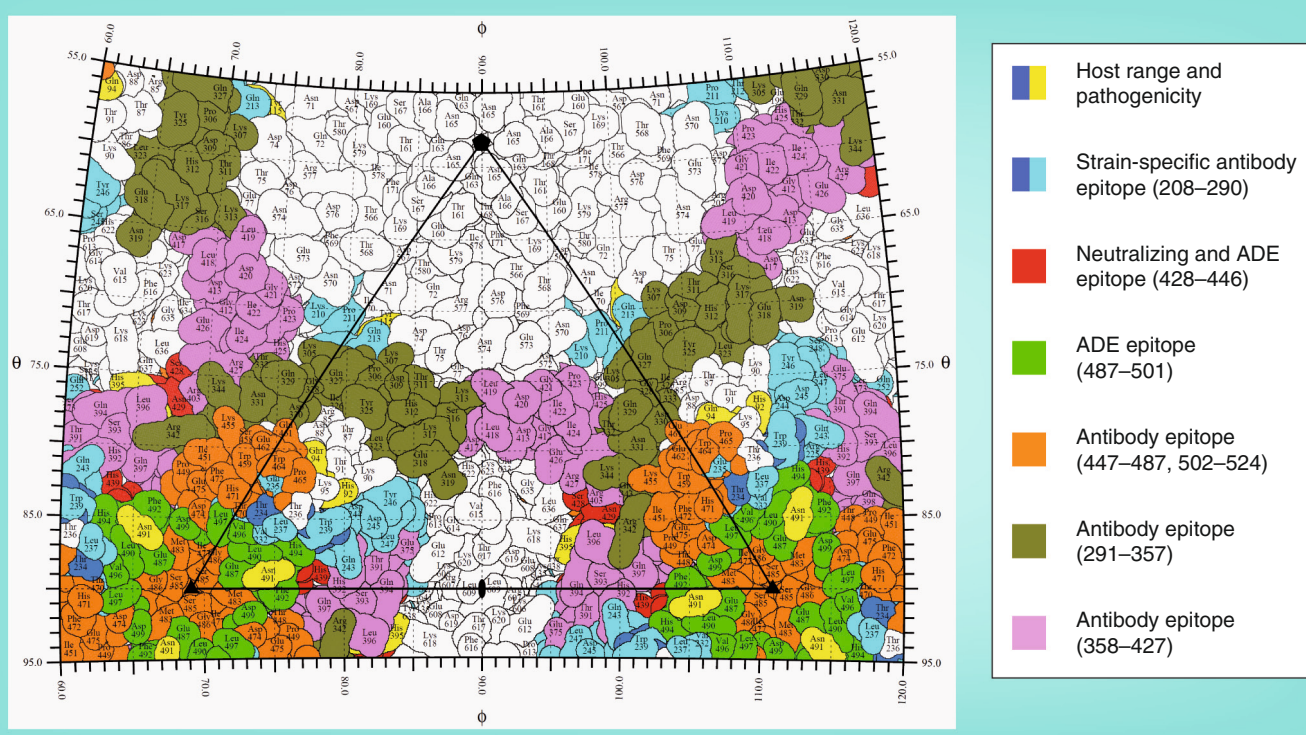


Figure 5. Stereographic roadmap projection of the surface residues of Aleutian mink disease virus. The image shows surface residues in a viral asymmetric unit for the pseudoatomic model of the Aleutian mink disease virus capsid visualized as described for adeno-associated virus serotype 2 in **FIGURE 4**. The colored residues show amino acids that are important determinants of host range, pathogenicity and antigenicity as indicated on the right-hand side. The coordinates were obtained as described in the legend of **FIGURE 2A**. Generated using the program RIVEM [245].
ADE: Antibody-dependent enhancement.

to isolated globoside *in vitro*. The structurally mapped globoside footprint includes residues Q399, Q400, Y401, T402, D403, Q404 and E406 (**FIGURE 6**). For the $\alpha_5\beta_1$ coreceptor, the binding site is not known, but the NGR motif of AAV2 is partially conserved as NTR (N323, T324, R325) (**FIGURE 6**). For MVM, mutagenesis and structural studies identified the two-fold depression as the SA binding site [191]. The binding pocket residues proximal to the SA are VP2 residues K241, M243, I362, K368, Y396, W398, D399, T401, F403, D553, Y558 and T578. Significantly, the residues determining *in vitro* tropism (317 and 321), conferring fibrotropism on MVMi (399, 460, 553 and 558), *in vivo* pathogenicity (325, 362 and 368), and those associated with the development of leukopenia (321, 551 and 575) are localized in the vicinity of this SA binding pocket (**FIGURE 7**). These residues are in VP VR4, VR5 and VR8 (**FIGURE 2A**) (defined in [172]). There is no information available for BPV1 capsid–receptor interactions. Where information is available, the sites utilized for receptor recognition or as determinants of tissue tropism and pathogenicity

by autonomous parvoviruses are only present on assembled capsids. Interestingly, different regions are utilized by the different viruses for receptor binding: the twofold depression (ADV and MVM) and the depression at the threefold axis (B19V) and threefold protrusions (ADV and CPV). The overlap between the receptor attachment sites and determinants of tissue tropism and pathogenicity for some of these viruses suggests a role for receptor interaction in these phenotypes.

Autonomous parvovirus capsid internalization & trafficking

Autonomous parvovirus capsid internalization is also proposed to occur via clathrin-mediated endocytosis following interaction with receptor molecules as discussed above for the AAVs, with pH-mediated capsid transitions, including the externalization of the VP1u, as well as components of the extracellular matrix being important for successful trafficking (reviewed in [22]). MVM, the best-characterized autonomous parvovirus with respect to cellular trafficking, will be the main focus of this section.

Exposure of MVM to the low pH of the endosome induces the externalization of the VP1u for its PLA₂ activity, essential for endosomal exit [30,192,193]. Mutagenesis studies with MVM, as has been done with AAV2, indicates that the channel at the fivefold axis also serves as the VP1u extrusion route [194,195]. By contrast, for B19V, where VP1u is reported to be always exposed on the capsid surface, externalization is not necessary for infection, although the PLA₂ sequence is still necessary [196,197]. B19V is, however, reported to be more sensitive to inactivation at low-pH conditions than other autonomous parvoviruses, including MVM [198]. Unlike the AAV transduction, where proteasome inhibitors enhance transduction [199], this treatment is detrimental to MVM (and CPV) infection, although particle ubiquitinylated or degradation has not been observed [20,200]. Specifically, the chymotrypsin-like activity of proteasome appears to be necessary. The capsids move through the cytoplasm by microtubule-mediated processes, as shown by the inhibitory effect of the microtubule depolymerizing drug, nocodazole, and antibodies to the motor protein dynein [20,21,201].

As discussed above for the AAVs, the exact mechanism of autonomous parvovirus capsid genome translocation into the nucleus is unclear. MVM capsid conformational shifts are reported to allow the exposure of the VP1 N-terminal that also contains NLSS required for nuclear trafficking [202,203]. There are reports that capsids can translocate through the nuclear pore complex, whereas other studies report that virus uncoating occurs in the endosomal pathway and the viral DNA enters the nucleus devoid of VP [193]. An alternative nuclear entry strategy involving partial disruption of the nuclear membrane by host caspase-3 has also been proposed [204–206].

Autonomous parvovirus capsid uncoating, genome replication, protein expression, capsid assembly, genome packaging & nuclear exit

The process of autonomous parvovirus capsid uncoating is yet to be fully defined, and again MVM is the best-characterized member with respect to capsid requirements. Studies with MVM suggest that the low endosomal pH and the low concentration of divalent cation concentration in the cytoplasm, together with

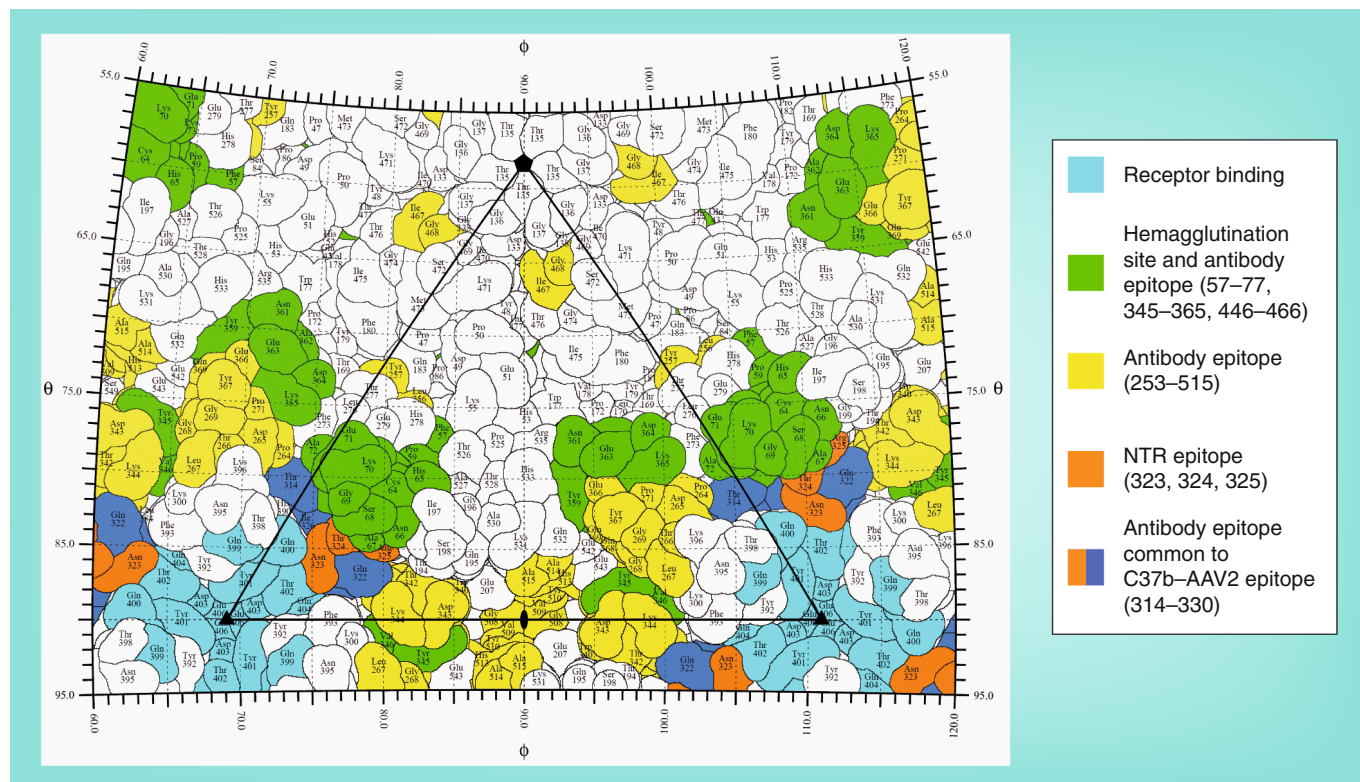


Figure 6. Stereographic roadmap projection of the surface residues of human parvovirus B19V. The image shows surface residues in a viral asymmetric unit for the atomic model of the human parvovirus B19V capsid visualized as described for adeno-associated virus serotype 2 in **FIGURE 4**. The colored residues show amino acids that are important determinants of receptor binding, hemagglutination and antigenicity as indicated on the right-hand side. Coordinates were obtained as described in the legend of **FIGURE 2A**. Generated using the program RIVEM [245].

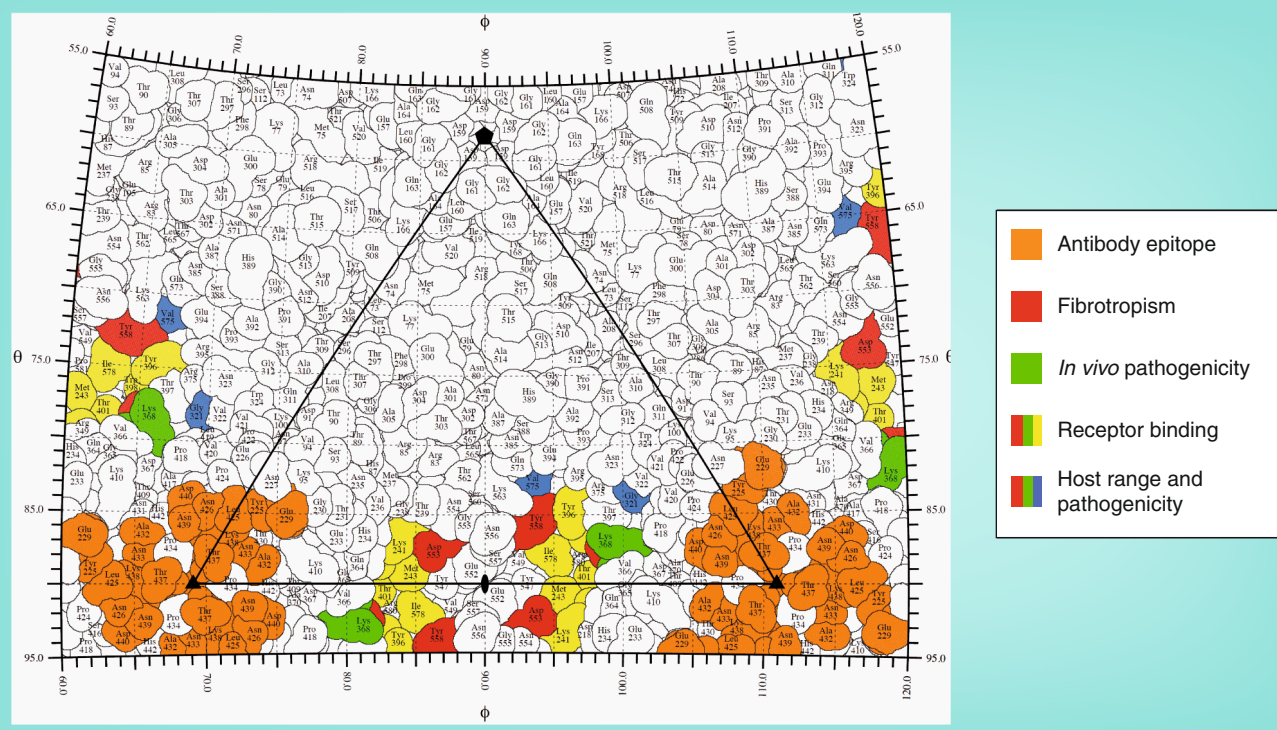


Figure 7. Stereographic roadmap projection of the surface residues of the prototype strain of minute virus of mice. The image shows surface residues in a viral asymmetric unit for the atomic model of the prototype strain of minute virus of mice capsid visualized as described for adeno-associated virus serotype 2 in **FIGURE 4**. The colored residues are important determinants of receptor binding, host range, pathogenicity and antigenicity as indicated on the right-hand side. Coordinates were obtained as described in the legend of **FIGURE 2A**. This figure was generated using the program RIVEM [245].

receptor binding, are likely triggers for genome release [207]. The pH dependence of the simultaneous externalization of VP1u and viral DNA from intact capsids without particle disassembly has been observed *in vivo* [193]. Similarly, the *in vitro* heat-induced transitions that expose the VP1u also expose the 3' end of the viral DNA to polymerases [194,203,208].

Similar to the essential role played by the Rep proteins in the AAVs, the autonomous parvovirus NS proteins are important for genome replication. NS1 (83 kDa) is a phosphoprotein that has helicase, ATPase, DNA-nicking and sequence-specific DNA-binding activities that are essential for replication, and it is also the major mediator of cytotoxicity (reviewed in [209]). NS2 (24 kDa) is also required for virus replication, cytotoxicity, nuclear egress of progeny virions and capsid assembly [210–213]. Following genome delivery, NS1-initiated replication proceeds via a series of duplex intermediates in a rolling-hairpin mechanism primed by replication origins at each end of the linear genome, similar to Rep-mediated replication of AAV genome [214]. The replicated genome is transcribed and then translated in the cytoplasm, and the VPs are reportedly

transported back into the nucleus in the form of intermediates for capsid assembly. Mutagenesis and structural studies suggest that VP trimers are the stable assembly intermediates for MVM capsids [215]. The NLS in the VP1 N-terminal region and the structural nuclear localization motif localized in the common β-barrel region of the capsid, target the expressed VPs to the nucleus [202,216]. Although VP1 shares the VP2 sequence, VP2 is reported to act like a chaperone and assists in VP1 folding and formation of trimers. The prediction is that once the correctly folded trimers enter the nucleus and assemble into empty capsids, the NLS of VP1 and nuclear localization motif of VP2 become hidden in the capsid interior.

MVM is also the best-characterized autonomous parvovirus with respect to genome packaging. DNA is reported to be packaged in a 3' to 5' direction into the preformed empty capsid using energy provided by NS1 [121,217]. Studies with capsid mutants that produce only empty particles suggest a role for VPs in packaging [218]. MVM, unlike the AAVs, packages only the negative strand of its ssDNA genome, which is complimentary to the mRNA. Some

autonomous parvoviruses package strands of both polarities in an equimolar ratio (e.g., LuIII) and **bocaviruses** (e.g., BPV1) package either polarity in different proportions [219]. It has been demonstrated using a MVM and LuIII chimeric virus that secondary structure elements, including stem-loops and guanine-rich regions, can interrupt packaging [220,221]. Similar to the AAVs, mutational analysis suggests that the fivefold channel is the genome encapsidation and extrusion portal [194,195,222,223]. Crystal structures of MVM and CPV infectious virions have shown the presence of ordered genomic ssDNA inside the capsid. The DNA-capsid interactions involve residues that surround the interior capsid surface near the two- and threefold axes [42,54]. However, unlike the AAVs for which ordered nucleotides are structurally observed even in 'empty' *Baculovirus* expressed capsids (see above), suggesting a role for nonspecific DNA interactions in capsid assembly, there is no ordered DNA in empty capsid structures in MVM or CPV. This suggests that the capsid–genome interactions in autonomous parvoviruses that may be associated with capsid assembly are specific. Consistently, autonomous parvoviruses are less tolerant of replacement of wild-type genome sequences, unlike the AAVs that can package foreign genes for vector production [224,225]. Once packaged, the high number of basic residues in the VP1 N-terminus, together with polyamines, has been suggested to neutralize the packaged genome.

The exit mechanism for the autonomous parvoviruses is also best characterized for MVM. For this and other members of the *Parvovirus* genus, the VP2 N-termini are internally disposed in empty capsids, but prior to, or coincident with, the beginning of DNA packaging, a structural shift occurs, leading to its exposure. The VP2 N-terminal extension possesses a phosphoserine-rich nuclear export signal that is reported to interact with the exportin molecule CRM1 in normal mouse fibroblasts to traffic packaged virions out of the nucleus [226,227]. Full (virions with packaged DNA) capsids are released from the cell with all their VP2 N-termini intact, but capsid maturation in the extracellular environment or during re-entry into a new host cell involves the proteolytic removal of approximately 25 amino acids from most of the VP2 N-termini to generate VP3, thus removing the nuclear export signal [194,227]. The exposure of VP2 for cleavage in virions can be mimicked by heat treatment [193,208,228].

Interestingly, although VP1 contains the same proteolytic cleavage site present in VP2, and the VP1 N-terminus is exposed in the same endosomal compartment as the VP2, it is still not cleaved. It is proposed that this may be due to a different pattern of phosphorylation between both polypeptides [226]. The fivefold channel is postulated to also serve as the site for VP2 externalization for cleavage to VP3 in autonomous parvoviruses that undergo a maturation step. For the members of the other autonomous parvovirus genera, little is known about their nuclear exit mechanism(s).

Autonomous parvovirus capsid-mediated antigenic response

Following egress from the host cell, the progeny virions are ready for a new round of infection and encounter neutralizing antibodies against the capsid and nonstructural proteins, a host defense mechanism that is essential for fighting against invading pathogenic microorganisms. As for the AAVs, both T-cell and B-cell antibody responses may be generated against autonomous parvovirus capsids, but the focus of this section will be the antibodies that recognize conformational epitopes on the capsid of the type members of the four genera.

Anti-ADV antibodies cause disease progression *in vivo* by Fc γ RII receptor-mediated enhanced uptake, but are also able to neutralize infectivity in CrFK cells *in vitro* and reduce the death rate in mink kits [229,230]. Immunodominant sites on the ADV capsid mapped by peptide studies are located on the wall between the two- and five-fold axes and on the shoulder and top of the threefold protrusion (FIGURE 5) [48,149,231]. VP residues from 208 to 524 are highly immunoreactive, and the stretch from 429 to 524 is the most immunodominant epitope and is localized on the protrusions (FIGURE 5). In addition, an ADV hypervariable region that spans residues 208–290 forms a strain-specific immunoreactive epitope that maps to the shoulder of the threefold protrusion. An antibody against VP2 peptide 428–446 is able to elicit ADV pathogenesis via aggregation of virus particles into immune complexes and mediates ADE. This antibody is also able to neutralize infectivity in CrFK cells. This epitope is located on the twofold wall and also includes residue 434 implicated in host range determination, tissue tropism and pathogenicity. Antibodies to this epitope are present in ADV-infected mink, and the neutralizing and ADE-mediating capability of such antibodies likely explains the failure

of capsid-based ADV vaccines [230,232]. Another epitope that spans residues 487–501, which is located on the wall of the threefold protrusion facing the axis (FIGURE 5), demonstrated limited ability to aggregate particles and induce ADE, but was non-neutralizing *in vitro*.

For B19V, the major antigenic response is elicited against the VP1u and the common VP2 region localized on the threefold protrusion is also immunogenic (FIGURE 6) [52,196,233,234]. Monoclonal antibodies E, L and 521-D recognize epitopes composed of VP2 residues 57–77, 345–365 and 446–466, respectively, and inhibit hemagglutination by B19V [235]. Peptide mapping studies also showed that antibodies against the short stretches of VP2 amino acids from 253 to 515 were neutralizing and these epitopes can be mapped to the two-/five-fold wall and to the base of the threefold protrusions (FIGURE 6) [233,234,236]. One of the B19V epitopes (VP2 residues 314–330) on the threefold protrusion overlaps the antigenic epitope of the AAV2 antibody C37-B that also blocks HS binding [141], an observation that is not too surprising given the similarity in surface topology of the viruses.

Epitope mapping for MVM has utilized natural variants or antibody therapy-selected escape mutants that no longer bind the neutralizing antibodies, in conjunction with the structural study of a capsid–antibody (Fab) complex by cryoreconstruction [237,238]. Long-term immune therapy with the neutralizing antibody B7 to protect mice from infection with MVMi resulted in the selection of escape mutants that had changes in residues 433–439 of VP2, which are located at the top of the threefold protrusion (FIGURE 7). Cryoreconstruction of MVMi complexed to the B7 antibody confirmed that the epitope and the residues in the footprint were 225, 228, 229, 425, 426 (parvovirus VR2 and VR4, FIGURE 2B) and loop 432–440 (FIGURE 7). This monoclonal antibody binds to all the three symmetry-related VPs and sterically inhibits the binding of more than one Fab per threefold protrusion. The mechanism of neutralization (i.e., the step in the life cycle affected by this antibody) is unknown.

Conclusion

The parvoviruses are assembled from 60 copies of essentially one capsid VP with unique N-terminal extensions in a few copies that perform specific tasks during infection. While many aspects of the infection process still remain to be fully understood, there is a significant amount of information available that

shows that the VP has evolved to assemble a capsid capable of performing all the specialist functions required for successful host cell infection. Variation in the capsid VP sequence and structure confer differences in surface topology which likely evolved from a need to enable host-specific interactions, resulting in the establishment of specific host cellular niches for each virus. The most pronounced capsid surface regions are also targets of the host immune antibody response, consistent with the need of the host to defend against invading pathogens. With respect to the dependoviruses, identifying these immunogenic regions and modifying them provides a means to engineer capsids capable of escaping host immune recognition while maintaining tropism towards improving their efficacy as gene delivery vectors. For the autonomous viruses with a pathogenic phenotype, information on antigenic regions aids the development of vaccines.

Future perspective

The *Parvoviridae* provide diversity by having pathogenic and nonpathogenic members in the same genus with minor sequence differences, and also members that circulate in human populations without being associated with any disease. The latter are being developed as gene therapy vectors. The ‘what next’ for this family will be the molecular elucidation of virus infection through structure–function annotation of the steps taken by the viruses during infection. Understanding the mechanism of host engagement and manipulation by these viruses will be fundamental for the developments of treatments, in the form of small molecule inhibitors or vaccines for emerging members, such as the HBoV, and the full realization of their utility as therapeutic gene delivery vectors for disease treatment.

The dream of the structural virologist is 3D visualization of cellular virus infection *in situ*. In the past decade, the field of structural virology has witnessed major advancements in the applications utilized for structural characterization, including improved computational power, x-ray free-electron laser data collection on a particle stream (not crystals) of a giant virus and the atomic resolution of large viruses using cryoreconstruction [239–241]. In addition, developments in live-cell microscopy and electron tomography are bringing us closer to the dream of visualizing infection in progress [242]. These developments provide the opportunity for continued functional annotation of the essential interactions required for *Parvoviridae* infection at atomic resolution and *in situ*.

Executive summary

Parvoviridae classification & structure

- The Parvoviridae are small ssDNA viruses packaged into nonenveloped T = 1 icosahedral capsids of approximately 260 Å in diameter.
- The Parvovirinae subfamily is divided into five genera: *Amdovirus*, *Bocavirus*, *Dependovirus*, *Erythrovirus* and *Parvovirus*.
- The structurally conserved viral protein (VP) assembles a capsid that plays a role in most of the steps involved in infection, including receptor recognition, virus trafficking to the nucleus, capsid assembly and genome packaging, and is the target of the host immune response.
- The fivefold channel is proposed to be the portal for several functions, including VP1u externalization for its PLA2 activity, genome packaging and VP2 externalization (in autonomous parvoviruses) for nuclear exit, although this remains to be confirmed.

Dependovirus

- The adeno-associated virus' (AAVs) are nonpathogenic and are under development as viral gene delivery vectors for the treatment of several genetic diseases.
- The AAVs utilize different glycans, such as heparan sulfate, sialic acid and galactose, as initial cell surface recognition molecules, although information is not available for all the serotypes.
- The threefold protrusion on the capsid is utilized for glycan receptor attachment.
- Several protein coreceptors are utilized for cellular internalization by AAV2, the best-characterized serotype. The sites for interaction are yet to be structurally confirmed.
- The AAV capsid is subject to endocytic pathway pH-mediated transitions.
- The exact mechanism of nuclear translocation, capsid uncoating and nuclear exit remain to be elucidated.
- The host immune response to AAV capsids, which neutralizes entry and post-entry steps in infection, is a major obstacle to gene delivery.

Autonomous parvoviruses

- The autonomous parvoviruses can cause lethal infections in young hosts.
- Given the available data, there is no clear distinction between primary cell recognition receptors and receptors that function to internalize virus capsids.
- The capsids utilize different regions of the capsid as receptor binding sites.
- Like the AAVs, the capsid undergoes transitions mediated by endocytic pHs.
- Like the AAVs, the exact mechanism of nuclear translocation and capsid uncoating is unclear. However, it is known that the genome is released in the 3' to 5' direction.
- Antibody binding to Aleutian mink disease virus capsids enhances infection in macrophages, resulting in failure of vaccine based treatments. Antibodies to other viruses are neutralizing by various mechanisms, including inhibition of receptor attachment and other infection steps still to be identified.

Acknowledgements

The authors would like to thank Bob Sinkovits for help in generating FIGURE 2B and FIGURE 3.

Financial & competing interests disclosure

NIH project R01 GM082946 and NSF project MCB-0718948 are acknowledged for support. The authors have no other relevant affiliations or financial involvement with any organization or entity with a financial interest in or financial conflict with the subject matter or materials discussed in the manuscript apart from those disclosed.

No writing assistance was utilized in the production of this manuscript.

References

Papers of special note have been highlighted as:

- of interest
 - of considerable interest
1. Berns KI, Parrish CR. *Parvoviridae*. In: *Field's Virology*. Knipe DM, Howley PM, Griffin DE et al. (Eds). Lippincott Williams & Wilkins, PA, USA, 2437–2478 (2007).
 2. Bergoin M, Kleinschmidt J, Almendral JM et al. Ninth report of the International Committee on Taxonomy of Viruses. In: *Virus Taxonomy*. King AMQ, Adams MJ, Carstens EB, Lefkowitz EJ (Eds). Elsevier, The Netherlands, 405–425 (2011).
 3. Parrish CR. Autonomous parvovirus variation and evolution. In: *Parvoviruses*. Kerr JR, Cotmore SF, Bloom ME, Linden RM, Parrish CR (Eds). Hodder Arnold, UK, 47–54 (2006).
 4. Brown KE. The genus *Erythrovirus*. In: *Parvoviruses*. Kerr JR, Cotmore SF, Bloom ME, Linden RM, Parrish CR (Eds). Hodder Arnold, UK, 25–46 (2006).
 5. Bowles DE, Rabinowitz JE, Samulski RJ. The genus *Dependovirus*. In: *Parvoviruses*. Kerr JR, Cotmore SF, Bloom ME, Linden RM, Parrish CR (Eds). Hodder Arnold, UK, 15–24 (2006).
 6. Cotmore SF, Tattersall R. Structure and organization of the viral genome. In: *Parvoviruses*. Kerr JR, Cotmore SF, Bloom ME, Linden RM, Parrish CR (Eds). Hodder Arnold, UK, 107–124 (2006).
 7. Chen KC, Shull BC, Moses EA, Lederman M, Stout ER, Bates RC. Complete nucleotide sequence and genome organization of bovine parvovirus. *J. Virol.* 60(3), 1085–1097 (1986).
 8. Sun Y, Chen AY, Cheng F, Guan W, Johnson FB, Qiu J. Molecular characterization of infectious clones of the minute virus of canines reveals unique features of bocaviruses. *J. Virol.* 83(8), 3956–3967 (2009).
 9. Lederman M, Bates RC, Stout ER. *In vitro* and *in vivo* studies of bovine parvovirus proteins. *J. Virol.* 48(1), 10–17 (1983).
 10. Johnson FB, Hoggan MD. Structural proteins of HADEN virus. *Virology* 51(1), 129–137 (1973).
 11. Chapman MS, Agbandje-McKenna M. Atomic structures of viral particles. In: *Parvoviruses*. Kerr JR, Cotmore SF, Bloom ME, Linden RM, Parrish CR (Eds). Hodder Arnold, UK, 107–124 (2006).

12. Bartlett JS, Wilcher R, Samulski RJ. Infectious entry pathway of adeno-associated virus and adeno-associated virus vectors. *J. Virol.* 74(6), 2777–2785 (2000).
13. Basak S, Turner H. Infectious entry pathway for canine parvovirus. *Virology* 186(2), 368–376 (1992).
- **Provided the first evidence that successful parvoviral infection requires trafficking through low pH endosomal compartments.**
14. Cotmore SF, Tattersall P. Parvoviral host range and cell entry mechanisms. *Adv. Virus Res.* 70, 183–232 (2007).
15. Duan D, Li Q, Kao AW, Yue Y, Pessin JE, Engelhardt JF. Dynamin is required for recombinant adeno-associated virus type 2 infection. *J. Virol.* 73(12), 10371–10376 (1999).
16. Parker JS, Parrish CR. Cellular uptake and infection by canine parvovirus involves rapid dynamin-regulated clathrin-mediated endocytosis, followed by slower intracellular trafficking. *J. Virol.* 74(4), 1919–1930 (2000).
17. Douar AM, Poulard K, Stockholm D, Danos O. Intracellular trafficking of adeno-associated virus vectors: routing to the late endosomal compartment and proteasome degradation. *J. Virol.* 75(4), 1824–1833 (2001).
- **First report of the proteasomal degradation of adeno-associated virus (AAV) during its infectious life cycle.**
18. Hansen J, Qing K, Srivastava A. Adeno-associated virus type 2-mediated gene transfer: altered endocytic processing enhances transduction efficiency in murine fibroblasts. *J. Virol.* 75(9), 4080–4090 (2001).
19. Parker JS, Murphy WJ, Wang D, O'Brien SJ, Parrish CR. Canine and feline parvoviruses can use human or feline transferrin receptors to bind, enter, and infect cells. *J. Virol.* 75(8), 3896–3902 (2001).
20. Ros C, Burckhardt CJ, Kempf C. Cytoplasmic trafficking of minute virus of mice: low-pH requirement, routing to late endosomes, and proteasome interaction. *J. Virol.* 76(24), 12634–12645 (2002).
21. Vihinen-Ranta M, Kalela A, Makinen P, Kakkola L, Marjomaki V, Vuento M. Intracellular route of canine parvovirus entry. *J. Virol.* 72(1), 802–806 (1998).
22. Harbison CE, Chiorini JA, Parrish CR. The parvovirus capsid odyssey: from the cell surface to the nucleus. *Trends Microbiol.* 16(5), 208–214 (2008).
23. Harbison CE, Lyi SM, Weichert WS, Parrish CR. Early steps in cell infection by parvoviruses: host-specific differences in cell receptor binding but similar endosomal trafficking. *J. Virol.* 83(20), 10504–10514 (2009).
24. Hueffer K, Palermo LM, Parrish CR. Parvovirus infection of cells by using variants of the feline transferrin receptor altering clathrin-mediated endocytosis, membrane domain localization, and capsid-binding domains. *J. Virol.* 78(11), 5601–5611 (2004).
25. Bantel-Schaal U, Hub B, Kartenbeck J. Endocytosis of adeno-associated virus type 5 leads to accumulation of virus particles in the Golgi compartment. *J. Virol.* 76(5), 2340–2349 (2002).
- **First description of an alternative trafficking pathway for an AAV.**
26. Boisvert M, Fernandes S, Tijsen P. Multiple pathways involved in porcine parvovirus cellular entry and trafficking toward the nucleus. *J. Virol.* 84(15), 7782–7792 (2010).
27. Johnson JS, Gentzsch M, Zhang L et al. AAV exploits subcellular stress associated with inflammation, endoplasmic reticulum expansion, and misfolded proteins in models of cystic fibrosis. *PLoS Pathog.* 7(5), E1002053 (2011).
- **The role of unfolded protein response in AAV trafficking.**
28. Agbandje-McKenna M, Chapman MS. Correlating structure with function in the viral capsid. In: *Parvoviruses*. Kerr JR, Cotmore SF, Bloom ME, Linden RM, Parrish CR (Eds). Hodder Arnold, UK, 125–140 (2006).
29. Agbandje-McKenna M, Kleinschmidt J. AAV capsid structure and cell interactions. *Methods Mol. Biol.* 807, 47–92 (2011).
- **Detailed review of the properties and structural characteristics of AAV as it relates to its life cycle.**
30. Zadori Z, Szelei J, Lacoste MC et al. A viral phospholipase A2 is required for parvovirus infectivity. *Dev. Cell* 1(2), 291–302 (2001).
- **Described the novel finding of an essential enzyme function, PLA₂, encoded within the VP1 N-terminus of parvoviruses. This VP1 unique region has since been demonstrated to be essential for infectivity.**
31. Sonntag F, Bleker S, Leuchs B, Fischer R, Kleinschmidt JA. Adeno-associated virus type 2 capsids with externalized VP1/VP2 trafficking domains are generated prior to passage through the cytoplasm and are maintained until uncoating occurs in the nucleus. *J. Virol.* 80(22), 11040–11054 (2006).
32. Wu P, Xiao W, Conlon T et al. Mutational analysis of the adeno-associated virus type 2 (AAV2) capsid gene and construction of AAV2 vectors with altered tropism. *J. Virol.* 74(18), 8635–8647 (2000).
33. Grieger JC, Snowdy S, Samulski RJ. Separate basic region motifs within the adeno-associated virus capsid proteins are essential for infectivity and assembly. *J. Virol.* 80(11), 5199–5210 (2006).
34. Johnson JS, Li C, Dippimo N, Weinberg MS, McCown TJ, Samulski RJ. Mutagenesis of adeno-associated virus type 2 capsid protein VP1 uncovers new roles for basic amino acids in trafficking and cell-specific transduction. *J. Virol.* 84(17), 8888–8902 (2010).
35. Xie Q, Lerch TF, Meyer NL, Chapman MS. Structure–function analysis of receptor-binding in adeno-associated virus serotype 6 (AAV-6). *Virology* 420(1), 10–19 (2011).
36. Ng R, Govindasamy L, Gurda BL et al. Structural characterization of the dual glycan binding adeno-associated virus serotype 6. *J. Virol.* 84(24), 12945–12957 (2010).
37. Lerch TF, Xie Q, Chapman MS. The structure of adeno-associated virus serotype 3B (AAV-3B): insights into receptor binding and immune evasion. *Virology* 403(1), 26–36 (2010).
38. Nam HJ, Lane MD, Padron E et al. Structure of adeno-associated virus serotype 8, a gene therapy vector. *J. Virol.* 81(22), 12260–12271 (2007).
39. Padron E, Bowman V, Kaludov N et al. Structure of adeno-associated virus type 4. *J. Virol.* 79(8), 5047–5058 (2005).
40. Walters RW, Agbandje-McKenna M, Bowman VD et al. Structure of adeno-associated virus serotype 5. *J. Virol.* 78(7), 3361–3371 (2004).
41. Xie Q, Bu W, Bhatia S et al. The atomic structure of adeno-associated virus (AAV-2), a vector for human gene therapy. *Proc. Natl Acad. Sci. USA* 99(16), 10405–10410 (2002).
42. Agbandje-McKenna M, Llamas-Saiz AL, Wang F, Tattersall P, Rossman MG. Functional implications of the structure of the murine parvovirus, minute virus of mice. *Structure* 6(11), 1369–1381 (1998).
43. Llamas-Saiz AL, Agbandje-McKenna M, Wikoff WR, Bratton J, Tattersall P, Rossman MG. Structure determination of minute virus of mice. *Acta Crystallogr. D Biol. Crystallogr.* 53(Pt 1), 93–102 (1997).
44. Wu H, Keller W, Rossman MG. Determination and refinement of the canine parvovirus empty-capsid structure. *Acta Crystallogr. D Biol. Crystallogr.* 49(Pt 6), 572–579 (1993).
45. Agbandje M, McKenna R, Rossman MG, Strassheim ML, Parrish CR. Structure determination of feline panleukopenia virus empty particles. *Proteins* 16(2), 155–171 (1993).

46. Kronenberg S, Bottcher B, Von Der Lieth CW, Bleker S, Kleinschmidt JA. A conformational change in the adeno-associated virus type 2 capsid leads to the exposure of hidden VP1 N termini. *J. Virol.* 79(9), 5296–5303 (2005).
47. Kronenberg S, Kleinschmidt JA, Bottcher B. Electron cryo-microscopy and image reconstruction of adeno-associated virus type 2 empty capsids. *EMBO Rep.* 2(11), 997–1002 (2001).
48. McKenna R, Olson NH, Chipman PR *et al.* Three-dimensional structure of Aleutian mink disease parvovirus: implications for disease pathogenicity. *J. Virol.* 73(8), 6882–6891 (1999).
49. Govindasamy L, Padron E, McKenna R *et al.* Structurally mapping the diverse phenotype of adeno-associated virus serotype 4. *J. Virol.* 80(23), 11556–11570 (2006).
- **Began the description of the regions of the AAV capsid that vary between the serotypes and began the functional annotation of these regions. They play essential roles in cell recognition, determine the serotype transduction efficiency and are the determinants of antigenic reactivity.**
50. Simpson AA, Hebert B, Sullivan GM *et al.* The structure of porcine parvovirus: comparison with related viruses. *J. Mol. Biol.* 315(5), 1189–1198 (2002).
51. Gurda BL, Parent KN, Bladek H *et al.* Human bocavirus capsid structure: insights into the structural repertoire of the parvoviridae. *J. Virol.* 84(12), 5880–5889 (2010).
52. Kaufmann B, Simpson AA, Rossmann MG. The structure of human parvovirus B19. *Proc. Natl Acad. Sci. USA* 101(32), 11628–11633 (2004).
53. Kaufmann B, Chipman PR, Kostyuchenko VA, Modrow S, Rossmann MG. Visualization of the externalized VP2 N termini of infectious human parvovirus B19. *J. Virol.* 82(15), 7306–7312 (2008).
54. Tsao J, Chapman MS, Agbandje M *et al.* The three-dimensional structure of canine parvovirus and its functional implications. *Science* 251(5000), 1456–1464 (1991).
- **The first crystal structure solved for a member of Parvoviridae family at 3.25-Å resolution by the heavy atom phasing method, which provided the first starting model for the structure determination of other members.**
55. Sonntag F, Kother K, Schmidt K *et al.* The assembly-activating protein promotes capsid assembly of different adeno-associated virus serotypes. *J. Virol.* 85(23), 12686–12697 (2011).
56. Hogan MD, Blacklow NR, Rowe WP. Studies of small DNA viruses found in various adenovirus preparations: physical, biological, and immunological characteristics. *Proc. Natl Acad. Sci. USA* 55(6), 1467–1474 (1966).
57. Atchison RW, Casto BC, Hammon WM. Adenovirus-associated defective virus particles. *Science* 149(3685), 754–756 (1965).
58. Carter BJ. Adeno-associated virus vectors and biology of gene delivery. In: *Parvoviruses*. Kerr JR, Cotmore SF, Bloom ME, Linden RM, Parrish CR (Eds). Hodder Arnold, UK, 497–498 (2006).
59. Mueller C, Flotte TR. Clinical gene therapy using recombinant adeno-associated virus vectors. *Gene Ther.* 15(11), 858–863 (2008).
60. Daya S, Berns KI. Gene therapy using adeno-associated virus vectors. *Clin. Microbiol. Rev.* 21(4), 583–593 (2008).
61. Coura Rdos S, Nardi NB. The state of the art of adeno-associated virus-based vectors in gene therapy. *Virol. J.* 4, 99 (2007).
62. Nathwani AC, Tuddenham EGD, Rangarajan S *et al.* Adenovirus-associated virus vector-mediated gene transfer in hemophilia B. *N. Engl. J. Med.* 365(25), 2357–2365 (2011).
63. Steiger K, Cronin T, Bennett J, Rolling F. Adeno-associated virus mediated gene therapy for retinal degenerative diseases. *Methods Mol. Biol.* 807, 179–218 (2011).
64. Michelfelder S, Trepel M. Adeno-associated viral vectors and their redirection to cell-type specific receptors. *Adv. Genet.* 67, 29–60 (2009).
65. Boutin S, Monteilhet V, Veron P *et al.* Prevalence of serum IgG and neutralizing factors against adeno-associated virus (AAV) types 1, 2, 5, 6, 8, and 9 in the healthy population: implications for gene therapy using AAV vectors. *Hum. Gene Ther.* 21(6), 704–712 (2010).
66. Gao G, Vandenberghe LH, Alvira MR *et al.* Clades of adeno-associated viruses are widely disseminated in human tissues. *J. Virol.* 78(12), 6381–6388 (2004).
67. Katano H, Afione S, Schmidt M, Chiorini JA. Identification of adeno-associated virus contamination in cell and virus stocks by PCR. *Biotechniques* 36(4), 676–680 (2004).
68. Qiu J, Cheng F, Pintel D. Molecular characterization of caprine adeno-associated virus (AAV-Go.1) reveals striking similarity to human AAV5. *Virology* 356(1–2), 208–216 (2006).
69. Arbetman AE, Lochrie M, Zhou S *et al.* Novel caprine adeno-associated virus (AAV) capsid (AAV-Go.1) is closely related to the primate AAV-5 and has unique tropism and neutralization properties. *J. Virol.* 79(24), 15238–15245 (2005).
70. Lochrie MA, Tatsuno GP, Arbetman AE *et al.* Adeno-associated virus (AAV) capsid genes isolated from rat and mouse liver genomic DNA define two new AAV species distantly related to AAV-5. *Virology* 353(1), 68–82 (2006).
71. Jacobson ER, Kopit W, Kennedy FA, Funk RS. Coinfection of a bearded dragon, *Pogona vitticeps*, with adenovirus- and dependovirus-like viruses. *Vet. Pathol.* 33(3), 343–346 (1996).
72. Zincarelli C, Solty S, Rengo G, Rabinowitz JE. Analysis of AAV serotypes 1–9 mediated gene expression and tropism in mice after systemic injection. *Mol. Ther.* 16(6), 1073–1080 (2008).
73. Liu X, Luo M, Guo C, Yan Z, Wang Y, Engelhardt JF. Comparative biology of rAAV transduction in ferret, pig and human airway epithelia. *Gene Ther.* 14(21), 1543–1548 (2007).
74. Limberis MP, Vandenberghe LH, Zhang L, Pickles RJ, Wilson JM. Transduction efficiencies of novel AAV vectors in mouse airway epithelium *in vivo* and human ciliated airway epithelium *in vitro*. *Mol. Ther.* 17(2), 294–301 (2009).
75. Li W, Zhang L, Johnson JS *et al.* Generation of novel AAV variants by directed evolution for improved CFTR delivery to human ciliated airway epithelium. *Mol. Ther.* 17(12), 2067–2077 (2009).
76. Akache B, Grimm D, Pandey K, Yant SR, Xu H, Kay MA. The 37/67-kilodalton laminin receptor is a receptor for adeno-associated virus serotypes 8, 2, 3, and 9. *J. Virol.* 80(19), 9831–9836 (2006).
77. Bell CL, Vandenberghe LH, Bell P *et al.* The AAV9 receptor and its modification to improve *in vivo* lung gene transfer in mice. *J. Clin. Invest.* 121(6), 2427–2435 (2011).
78. Di Pasquale G, Davidson BL, Stein CS *et al.* Identification of PDGFR as a receptor for AAV-5 transduction. *Nat. Med.* 9(10), 1306–1312 (2003).
79. Di Pasquale G, Kaludov N, Agbandje-McKenna M, Chiorini JA. BAAV transcytosis requires an interaction with beta-1–4 linked-glucosamine and gp96. *PLoS One* 5(3), E9336 (2010).
80. Dickey DD, Excoffon KJ, Koerber JT *et al.* Enhanced sialic acid-dependent endocytosis explains the increased efficiency of infection of airway epithelia by a novel adeno-associated virus. *J. Virol.* 85(17), 9023–9030 (2011).

81. Kashiwakura Y, Tamayose K, Iwabuchi K *et al.* Hepatocyte growth factor receptor is a coreceptor for adeno-associated virus type 2 infection. *J. Virol.* 79(1), 609–614 (2005).
82. Ling C, Lu Y, Kalsi JK *et al.* Human hepatocyte growth factor receptor is a cellular coreceptor for adeno-associated virus serotype 3. *Hum. Gene Ther.* 21(12), 1741–1747 (2010).
83. Qing K, Mah C, Hansen J, Zhou S, Dwarki V, Srivastava A. Human fibroblast growth factor receptor 1 is a co-receptor for infection by adeno-associated virus 2. *Nat. Med.* 5(1), 71–77 (1999).
84. Seiler MP, Miller AD, Zabner J, Halbert CL. Adeno-associated virus types 5 and 6 use distinct receptors for cell entry. *Hum. Gene Ther.* 17(1), 10–19 (2006).
85. Shen S, Bryant KD, Brown SM, Randell SH, Asokan A. Terminal N-linked galactose is the primary receptor for adeno-associated virus 9. *J. Biol. Chem.* 286(15), 13532–13540 (2011).
86. Summerford C, Bartlett JS, Samulski RJ. AlphaVbeta5 integrin: a co-receptor for adeno-associated virus type 2 infection. *Nat. Med.* 5(1), 78–82 (1999).
87. Summerford C, Samulski RJ. Membrane-associated heparan sulfate proteoglycan is a receptor for adeno-associated virus type 2 virions. *J. Virol.* 72(2), 1438–1445 (1998).
- Identification of heparan sulfate proteoglycan as AAV2 receptor, which is now used as a purification reagent.**
88. Walters RW, Yi SM, Keshavjee S *et al.* Binding of adeno-associated virus type 5 to 2,3-linked sialic acid is required for gene transfer. *J. Biol. Chem.* 276(23), 20610–20616 (2001).
89. Weller ML, Amornphimoltham P, Schmidt M, Wilson PA, Gutkind JS, Chiorini JA. Epidermal growth factor receptor is a co-receptor for adeno-associated virus serotype 6. *Nat. Med.* 16(6), 662–664 (2010).
90. Wu Z, Miller E, Agbandje-McKenna M, Samulski RJ. Alpha2,3 and alpha2,6 N-linked sialic acids facilitate efficient binding and transduction by adeno-associated virus types 1 and 6. *J. Virol.* 80(18), 9093–9103 (2006).
91. Wu Z, Asokan A, Grieger JC, Govindasamy L, Agbandje-McKenna M, Samulski RJ. Single amino acid changes can influence titer, heparin binding, and tissue tropism in different adeno-associated virus serotypes. *J. Virol.* 80(22), 11393–11397 (2006).
92. Asokan A, Hamra JB, Govindasamy L, Agbandje-McKenna M, Samulski RJ. Adeno-associated virus type 2 contains an integrin alpha5beta1 binding domain essential for viral cell entry. *J. Virol.* 80(18), 8961–8969 (2006).
93. Kaludov N, Brown KE, Walters RW, Zabner J, Chiorini JA. Adeno-associated virus serotype 4 (AAV4) and AAV5 both require sialic acid binding for hemagglutination and efficient transduction but differ in sialic acid linkage specificity. *J. Virol.* 75(15), 6884–6893 (2001).
94. Blackburn SD, Cline SE, Hemming JP, Johnson FB. Attachment of bovine parvovirus to O-linked alpha 2,3 neuraminic acid on glycophorin A. *Arch. Virol.* 150(7), 1477–1484 (2005).
95. O'Donnell J, Taylor KA, Chapman MS. Adeno-associated virus-2 and its primary cellular receptor – cryo-EM structure of a heparin complex. *Virology* 385(2), 434–443 (2009).
96. Levy HC, Bowman VD, Govindasamy L *et al.* Heparin binding induces conformational changes in adeno-associated virus serotype 2. *J. Struct. Biol.* 165(3), 146–156 (2009).
97. Schmidt M, Chiorini JA. Gangliosides are essential for bovine adeno-associated virus entry. *J. Virol.* 80(11), 5516–5522 (2006).
98. Opie SR, Warrington KH Jr, Agbandje-McKenna M, Zolotukhin S, Muzyczka N. Identification of amino acid residues in the capsid proteins of adeno-associated virus type 2 that contribute to heparan sulfate proteoglycan binding. *J. Virol.* 77(12), 6995–7006 (2003).
99. Kern A, Schmidt K, Leder C *et al.* Identification of a heparin-binding motif on adeno-associated virus type 2 capsids. *J. Virol.* 77(20), 11072–11081 (2003).
100. Excoffon KJ, Koerber JT, Dickey DD *et al.* Directed evolution of adeno-associated virus to an infectious respiratory virus. *Proc. Natl Acad. Sci. USA* 106(10), 3865–3870 (2009).
101. Blackburn SD, Steadman RA, Johnson FB. Attachment of adeno-associated virus type 3H to fibroblast growth factor receptor 1. *Arch. Virol.* 151(3), 617–623 (2006).
102. Uhrig S, Coutelle O, Wiehe T, Perabo L, Hallek M, Buning H. Successful target cell transduction of capsid-engineered rAAV vectors requires clathrin-dependent endocytosis. *Gene Ther.* doi:10.1038/gt.2011.78 (2011) (Epub ahead of print).
103. Duan D, Yue Y, Yan Z, Yang J, Engelhardt JF. Endosomal processing limits gene transfer to polarized airway epithelia by adeno-associated virus. *J. Clin. Invest.* 105(11), 1573–1587 (2000).
104. Stahnke S, Lux K, Uhrig S *et al.* Intrinsic phospholipase A2 activity of adeno-associated virus is involved in endosomal escape of incoming particles. *Virology* 409(1), 77–83 (2011).
105. Bleker S, Sonntag F, Kleinschmidt JA. Mutational analysis of narrow pores at the fivefold symmetry axes of adeno-associated virus type 2 capsids reveals a dual role in genome packaging and activation of phospholipase A2 activity. *J. Virol.* 79(4), 2528–2540 (2005).
106. Bantel-Schaal U, Braspenning-Wesch I, Kartenbeck J. Adeno-associated virus type 5 exploits two different entry pathways in human embryo fibroblasts. *J. Gen. Virol.* 90(Pt 2), 317–322 (2009).
107. Nam HJ, Gurda BL, McKenna R *et al.* Structural studies of adeno-associated virus serotype 8 capsid transitions associated with endosomal trafficking. *J. Virol.* 85(22), 11791–11799 (2011).
- Structural insights into low pH-mediated capsid conformation transitions that likely prime the AAV capsid for subsequent events in trafficking and uncoating in the host nucleus.**
108. Olia AS, Prevelige PE Jr, Johnson JE, Cingolani G. Three-dimensional structure of a viral genome-delivery portal vertex. *Nat. Struct. Mol. Biol.* 18(5), 597–603 (2011).
109. Ros C, Baltzer C, Mani B, Kempf C. Parvovirus uncoating *in vitro* reveals a mechanism of DNA release without capsid disassembly and striking differences in encapsidated DNA stability. *Virology* 345(1), 137–147 (2006).
110. Zhong L, Li B, Jayandharan G *et al.* Tyrosine-phosphorylation of AAV2 vectors and its consequences on viral intracellular trafficking and transgene expression. *Virology* 381(2), 194–202 (2008).
111. Zhong L, Li B, Mah CS *et al.* Next generation of adeno-associated virus 2 vectors: point mutations in tyrosines lead to high-efficiency transduction at lower doses. *Proc. Natl Acad. Sci. USA* 105(22), 7827–7832 (2008).
112. Xiao W, Warrington KH Jr, Hearing P, Hughes J, Muzyczka N. Adenovirus-facilitated nuclear translocation of adeno-associated virus type 2. *J. Virol.* 76(22), 11505–11517 (2002).
113. Hansen J, Qing K, Srivastava A. Infection of purified nuclei by adeno-associated virus 2. *Mol. Ther.* 4(4), 289–296 (2001).
114. Sanlioglu S, Benson PK, Yang J, Atkinson EM, Reynolds T, Engelhardt JF. Endocytosis and nuclear trafficking of adeno-associated virus type 2 are controlled by rac1 and phosphatidylinositol-3 kinase activation. *J. Virol.* 74(19), 9184–9196 (2000).

115. Johnson JS, Samulski RJ. Enhancement of adeno-associated virus infection by mobilizing capsids into and out of the nucleolus. *J. Virol.* 83(6), 2632–2644 (2009).
116. Lux K, Goerlitz N, Schlemminger S *et al.* Green fluorescent protein-tagged adeno-associated virus particles allow the study of cytosolic and nuclear trafficking. *J. Virol.* 79(18), 11776–11787 (2005).
117. Cotmore SF, Tattersall R. A rolling-hairpin strategy: basic mechanism of DNA replication in the parvoviruses. In: *Parvoviruses*. Kerr JR, Cotmore SF, Bloom ME, Linden RM, Parrish CR (Eds). Hodder Arnold, UK, 171–188 (2006).
118. Walker SL, Wonderling RS, Owens RA. Mutational analysis of the adeno-associated virus type 2 Rep68 protein helicase motifs. *J. Virol.* 71(9), 6996–7004 (1997).
119. McCarty DM, Ni TH, Muzyczka N. Analysis of mutations in adeno-associated virus Rep protein *in vivo* and *in vitro*. *J. Virol.* 66(7), 4050–4057 (1992).
120. Chejanovsky N, Carter BJ. Mutation of a consensus purine nucleotide binding site in the adeno-associated virus *rep* gene generates a dominant negative phenotype for DNA replication. *J. Virol.* 64(4), 1764–1770 (1990).
121. King JA, Dubielzig R, Grimm D, Kleinschmidt JA. DNA helicase-mediated packaging of adeno-associated virus type 2 genomes into preformed capsids. *EMBO J.* 20(12), 3282–3291 (2001).
122. Ni TH, Zhou X, McCarty DM, Zolotukhin I, Muzyczka N. *In vitro* replication of adeno-associated virus DNA. *J. Virol.* 68(2), 1128–1138 (1994).
123. Dubielzig R, King JA, Weger S, Kern A, Kleinschmidt JA. Adeno-associated virus type 2 protein interactions: formation of pre-encapsidation complexes. *J. Virol.* 73(11), 8989–8998 (1999).
124. Bleker S, Pawlita M, Kleinschmidt JA. Impact of capsid conformation and Rep–capsid interactions on adeno-associated virus type 2 genome packaging. *J. Virol.* 80(2), 810–820 (2006).
125. Sonntag F, Schmidt K, Kleinschmidt JA. A viral assembly factor promotes AAV2 capsid formation in the nucleolus. *Proc. Natl Acad. Sci. USA* 107(22), 10220–10225 (2010).
- Reports the discovery of an assembly-activating protein that is essential for capsid assembly.
126. Diprimio N, Asokan A, Govindasamy L, Agbandje-McKenna M, Samulski RJ. Surface loop dynamics in adeno-associated virus capsid assembly. *J. Virol.* 82(11), 5178–5189 (2008).
127. Chejanovsky N, Carter BJ. Mutagenesis of an AUG codon in the adeno-associated virus rep gene: effects on viral DNA replication. *Virology* 173(1), 120–128 (1989).
128. Collaco RF, Kalman-Maltese V, Smith AD, Dignam JD, Trempe JP. A biochemical characterization of the adeno-associated virus Rep40 helicase. *J. Biol. Chem.* 278(36), 34011–34017 (2003).
129. Owens RA, Weitzman MD, Kyostio SR, Carter BJ. Identification of a DNA-binding domain in the amino terminus of adeno-associated virus Rep proteins. *J. Virol.* 67(2), 997–1005 (1993).
130. Yang Q, Trempe JP. Analysis of the terminal repeat binding abilities of mutant adeno-associated virus replication proteins. *J. Virol.* 67(7), 4442–4447 (1993).
131. McCarty DM, Pereira DJ, Zolotukhin I, Zhou X, Ryan JH, Muzyczka N. Identification of linear DNA sequences that specifically bind the adeno-associated virus Rep protein. *J. Virol.* 68(8), 4988–4997 (1994).
132. Yoon-Robarts M, Linden RM. Identification of active site residues of the adeno-associated virus type 2 Rep endonuclease. *J. Biol. Chem.* 278(7), 4912–4918 (2003).
133. Mansilla-Soto J, Yoon-Robarts M, Rice WJ, Arya S, Escalante CR, Linden RM. DNA structure modulates the oligomerization properties of the AAV initiator protein Rep68. *PLoS Pathog.* 5(7), e1000513 (2009).
134. Timpe J, Bevington J, Casper J, Dignam JD, Trempe JP. Mechanisms of adeno-associated virus genome encapsidation. *Curr. Gene Ther.* 5(3), 273–284 (2005).
135. Herzog RW. Immune responses to AAV capsid: are mice not humans after all? *Mol. Ther.* 15(4), 649–650 (2007).
136. Sabatino DE, Mingozzi F, Hui DJ *et al.* Identification of mouse AAV capsid-specific CD8⁺ T cell epitopes. *Mol. Ther.* 12(6), 1023–1033 (2005).
137. Mays LE, Wilson JM. Identification of the murine AAVrh32.33 capsid-specific CD8⁺ T cell epitopes. *J. Gene Med.* 11(12), 1095–1102 (2009).
138. Li C, Hirsch M, Diprimio N *et al.* Cytotoxic-T-lymphocyte-mediated elimination of target cells transduced with engineered adeno-associated virus type 2 vector *in vivo*. *J. Virol.* 83(13), 6817–6824 (2009).
139. Manno CS, Pierce GF, Arruda VR *et al.* Successful transduction of liver in hemophilia by AAV-Factor IX and limitations imposed by the host immune response. *Nat. Med.* 12(3), 342–347 (2006).
140. Zaiss AK, Muruve DA. Immunity to adeno-associated virus vectors in animals and humans: a continued challenge. *Gene Ther.* 15(11), 808–816 (2008).
141. Wobus CE, Hugle-Dorr B, Girod A, Petersen G, Hallek M, Kleinschmidt JA. Monoclonal antibodies against the adeno-associated virus type 2 (AAV-2) capsid: epitope mapping and identification of capsid domains involved in AAV-2-cell interaction and neutralization of AAV-2 infection. *J. Virol.* 74(19), 9281–9293 (2000).
- This antibody epitope mapping study identified immunodominant AAV2 capsid regions and provided reagents that have impacted the field with respect to further immunological studies of AAVs.
142. Lochrie MA, Tatsuno GP, Christie B *et al.* Mutations on the external surfaces of adeno-associated virus type 2 capsids that affect transduction and neutralization. *J. Virol.* 80(2), 821–834 (2006).
- An exhaustive mutagenesis study of AAV2 capsid surface-exposed residues to elucidate the role played by the capsid in various steps of viral life cycle, including receptor attachment and antibody recognition.
143. Kuck D, Kern A, Kleinschmidt JA. Development of AAV serotype-specific ELISAs using novel monoclonal antibodies. *J. Virol. Methods* 140(1–2), 17–24 (2007).
144. Harbison CE, Weichert WS, Gurda BL, Chiorini JA, Agbandje-McKenna M, Parrish CR. Examining the cross-reactivity and neutralization mechanisms of a panel of monoclonal antibodies against adeno-associated virus serotypes 1 and 5. *J. Gen. Virol.* 93(Pt 2), 347–355 (2012).
145. Weitzman MD. The parvovirus life cycle: an introduction to molecular interactions important for infection. In: *Parvoviruses*. Kerr JR, Cotmore SF, Bloom ME, Linden RM, Parrish CR (Eds). Hodder Arnold, UK, 143–156 (2006).
146. Tattersall P. The evolution of parvovirus taxonomy. In: *Parvoviruses*. Kerr JR, Cotmore SF, Bloom ME, Linden RM, Parrish CR (Eds). Hodder Arnold, UK, 5–14 (2006).
147. Bloom ME, Kanno H, Mori S, Wolfenbarger JB. Aleutian mink disease: puzzles and paradigms. *Infect. Agents Dis.* 3(6), 279–301 (1994).
148. Dworak LJ, Wolfenbarger JB, Bloom ME. Aleutian mink disease parvovirus infection of K562 cells is antibody-dependent and is mediated via an Fc(gamma)RII receptor. *Arch. Virol.* 142(2), 363–373 (1997).

149. Bloom ME, Best SM, Hayes SF *et al.* Identification of Aleutian mink disease parvovirus capsid sequences mediating antibody-dependent enhancement of infection, virus neutralization, and immune complex formation. *J. Virol.* 75(22), 11116–11127 (2001).
150. Chareonsirisuthigul T, Kalayanarooj S, Ubol S. Dengue virus (DENV) antibody-dependent enhancement of infection upregulates the production of anti-inflammatory cytokines, but suppresses anti-DENV free radical and pro-inflammatory cytokine production, in THP-1 cells. *J. Gen. Virol.* 88(Pt 2), 365–375 (2007).
151. Munakata Y, Kato I, Saito T, Kodera T, Ishii KK, Sasaki T. Human parvovirus B19 infection of monocytic cell line U937 and antibody-dependent enhancement. *Virology* 345(1), 251–257 (2006).
152. Manteufel J, Truyen U. Animal bocaviruses: a brief review. *Intervirology* 51(5), 328–334 (2008).
153. Allander T. Human bocavirus. *J. Clin. Virol.* 41(1), 29–33 (2008).
154. Allander T, Jartti T, Gupta S *et al.* Human bocavirus and acute wheezing in children. *Clin. Infect. Dis.* 44(7), 904–910 (2007).
155. Allander T, Tammi MT, Eriksson M, Bjerkner A, Tiveljung-Lindell A, Andersson B. Cloning of a human parvovirus by molecular screening of respiratory tract samples. *Proc. Natl Acad. Sci. USA* 102(36), 12891–12896 (2005).
156. Arthur JL, Higgins GD, Davidson GP, Givney RC, Ratcliff RM. A novel bocavirus associated with acute gastroenteritis in Australian children. *PLoS Pathog.* 5(4), E1000391 (2009).
157. Lindner J, Karalar L, Schimanski S, Pfister H, Struff W, Modrow S. Clinical and epidemiological aspects of human bocavirus infection. *J. Clin. Virol.* 43(4), 391–395 (2008).
158. Vicente D, Cilla G, Montes M, Perez-Yarza EG, Perez-Trallero E. Human bocavirus, a respiratory and enteric virus. *Emerg. Infect. Dis.* 13(4), 636–637 (2007).
159. Chow BD, Ou Z, Esper FP. Newly recognized bocaviruses (HBoV, HBoV2) in children and adults with gastrointestinal illness in the United States. *J. Clin. Virol.* 47(2), 143–147 (2010).
160. Anderson MJ, Jones SE, Fisher-Hoch SP *et al.* Human parvovirus, the cause of erythema infectiosum (fifth disease)? *Lancet* 1(8338), 1378 (1983).
161. Katz VL, Chescheir NC, Bethea M. Hydrops fetalis from B19 parvovirus infection. *J. Perinatol.* 10(4), 366–368 (1990).
162. Naidoo SJ. Infection with Parvovirus B19. *Curr. Infect. Dis. Rep.* 1(3), 273–278 (1999).
163. Smith-Whitley K, Zhao H, Hodinka RL *et al.* Epidemiology of human parvovirus B19 in children with sickle cell disease. *Blood* 103(2), 422–427 (2004).
164. Young NS, Brown KE. Parvovirus B19. *N. Engl. J. Med.* 350(6), 586–597 (2004).
165. Green SW, Malkovska I, O'Sullivan MG, Brown KE. Rhesus and pig-tailed macaque parvoviruses: identification of two new members of the erythrovirus genus in monkeys. *Virology* 269(1), 105–112 (2000).
166. Segovia JC, Gallego JM, Bueren JA, Almendral JM. Severe leukopenia and dysregulated erythropoiesis in SCID mice persistently infected with the parvovirus minute virus of mice. *J. Virol.* 73(3), 1774–1784 (1999).
167. Kimsey PB, Engers HD, Hirt B, Jongeneel CV. Pathogenicity of fibroblast- and lymphocyte-specific variants of minute virus of mice. *J. Virol.* 59(1), 8–13 (1986).
168. Tattersall P, Bratton J. Reciprocal productive and restrictive virus-cell interactions of immunosuppressive and prototype strains of minute virus of mice. *J. Virol.* 46(3), 944–955 (1983).
169. Spegelaere P, Van Hille B, Spruyt N, Faisst S, Cornelis JJ, Rommelaeere J. Initiation of transcription from the minute virus of mice P4 promoter is stimulated in rat cells expressing a *c-Ha-ras* oncogene. *J. Virol.* 65(9), 4919–4928 (1991).
170. Paglino J, Tattersall P. The parvoviral capsid controls an intracellular phase of infection essential for efficient killing of stepwise-transformed human fibroblasts. *Virology* 416(1–2), 32–41 (2011).
171. Abschuetz A, Kehl T, Geibig R, Leuchs B, Rommelaeere J, Regnier-Vigouroux A. Oncolytic murine autonomous parvovirus, a candidate vector for glioma gene therapy, is innocuous to normal and immunocompetent mouse glial cells. *Cell Tissue Res.* 325(3), 423–436 (2006).
172. Kontou M, Govindasamy L, Nam HJ *et al.* Structural determinants of tissue tropism and *in vivo* pathogenicity for the parvovirus minute virus of mice. *J. Virol.* 79(17), 10931–10943 (2005).
173. Fox JM, Bloom ME. Identification of a cell surface protein from Crandell feline kidney cells that specifically binds Aleutian mink disease parvovirus. *J. Virol.* 73(5), 3835–3842 (1999).
174. Thacker TC, Johnson FB. Binding of bovine parvovirus to erythrocyte membrane sialylglycoproteins. *J. Gen. Virol.* 79(Pt 9), 2163–2169 (1998).
175. Brown KE, Anderson SM, Young NS. Erythrocyte P antigen: cellular receptor for B19 parvovirus. *Science* 262(5130), 114–117 (1993).
176. Weigel-Kelley KA, Yoder MC, Srivastava A. Alpha5beta1 integrin as a cellular coreceptor for human parvovirus B19: requirement of functional activation of beta1 integrin for viral entry. *Blood* 102(12), 3927–3933 (2003).
177. Munakata Y, Saito-Ito T, Kumura-Ishii K *et al.* Ku80 autoantigen as a cellular coreceptor for human parvovirus B19 infection. *Blood* 106(10), 3449–3456 (2005).
178. Cotmore SF, Tattersall P. The autonomously replicating parvoviruses of vertebrates. *Adv. Virus Res.* 33, 91–174 (1987).
- **The first comprehensive review on the autonomous parvoviruses.**
179. Kannagi R. Molecular mechanism for cancer-associated induction of sialyl Lewis X and sialyl Lewis A expression – the Warburg effect revisited. *Glycoconj. J.* 20(5), 353–364 (2004).
180. Nam HJ, Gurda-Whitaker B, Gan WY *et al.* Identification of the sialic acid structures recognized by minute virus of mice and the role of binding affinity in virulence adaptation. *J. Biol. Chem.* 281(35), 25670–25677 (2006).
181. Sato C, Fukuoka H, Ohta K *et al.* Frequent occurrence of pre-existing alpha 2 → 8-linked disialic and oligosialic acids with chain lengths up to 7 Sia residues in mammalian brain glycoproteins. Prevalence revealed by highly sensitive chemical methods and anti-di-, oligo-, and poly-Sia antibodies specific for defined chain lengths. *J. Biol. Chem.* 275(20), 15422–15431 (2000).
182. Hueffer K, Parker JS, Weichert WS, Geisel RE, Sgro JY, Parrish CR. The natural host range shift and subsequent evolution of canine parvovirus resulted from virus-specific binding to the canine transferrin receptor. *J. Virol.* 77(3), 1718–1726 (2003).
183. Barbis DP, Chang SF, Parrish CR. Mutations adjacent to the dimple of the canine parvovirus capsid structure affect sialic acid binding. *Virology* 191(1), 301–308 (1992).
184. Bloom ME, Andersen S, Perryman S, Lechner D, Wolfenbarger JB. Nucleotide sequence and genomic organization of Aleutian mink disease parvovirus (ADV): sequence comparisons between a nonpathogenic and a pathogenic strain of ADV. *J. Virol.* 62(8), 2903–2915 (1988).
185. Stevenson MA, Fox JM, Wolfenbarger JB, Bloom ME. Effect of a valine residue at codon 352 of the VP2 capsid protein on *in vivo* replication and pathogenesis of Aleutian disease parvovirus in mink. *Am. J. Vet. Res.* 62(10), 1658–1663 (2001).

186. Govindasamy L, Hueffer K, Parrish CR, Agbandje-McKenna M. Structures of host range-controlling regions of the capsids of canine and feline parvoviruses and mutants. *J. Virol.* 77(22), 12211–12221 (2003).
187. Hueffer K, Govindasamy L, Agbandje-McKenna M, Parrish CR. Combinations of two capsid regions controlling canine host range determine canine transferrin receptor binding by canine and feline parvoviruses. *J. Virol.* 77(18), 10099–10105 (2003).
188. Hafenstein S, Palermo LM, Kostyuchenko VA *et al.* Asymmetric binding of transferrin receptor to parvovirus capsids. *Proc. Natl Acad. Sci. USA* 104(16), 6585–6589 (2007).
189. Chipman PR, Agbandje-McKenna M, Kajigaya S *et al.* Cryo-electron microscopy studies of empty capsids of human parvovirus B19 complexed with its cellular receptor. *Proc. Natl Acad. Sci. USA* 93(15), 7502–7506 (1996).
- **First cryoreconstruction study that enabled the visualization of a capsid–receptor interaction.**
190. Kaufmann B, Baxa U, Chipman PR, Rossmann MG, Modrow S, Seckler R. Parvovirus B19 does not bind to membrane-associated globoside *in vitro*. *Virology* 332(1), 189–198 (2005).
191. Lopez-Bueno A, Rubio MP, Bryant N, McKenna R, Agbandje-McKenna M, Almendral JM. Host-selected amino acid changes at the sialic acid binding pocket of the parvovirus capsid modulate cell binding affinity and determine virulence. *J. Virol.* 80(3), 1563–1573 (2006).
- **First crystal structure of parvovirus–receptor complex identifying a sialic acid binding pocket.**
192. Farr GA, Zhang LG, Tattersall P. Parvoviral virions deploy a capsid-tethered lipolytic enzyme to breach the endosomal membrane during cell entry. *Proc. Natl Acad. Sci. USA* 102(47), 17148–17153 (2005).
193. Mani B, Baltzer C, Valle N, Almendral JM, Kempf C, Ros C. Low pH-dependent endosomal processing of the incoming parvovirus minute virus of mice virion leads to externalization of the VP1 N-terminal sequence (N-VP1), N-VP2 cleavage, and uncoating of the full-length genome. *J. Virol.* 80(2), 1015–1024 (2006).
194. Farr GA, Cotmore SF, Tattersall P. VP2 cleavage and the leucine ring at the base of the fivefold cylinder control pH-dependent externalization of both the VP1 N terminus and the genome of minute virus of mice. *J. Virol.* 80(1), 161–171 (2006).
195. Farr GA, Tattersall P. A conserved leucine that constricts the pore through the capsid fivefold cylinder plays a central role in parvoviral infection. *Virology* 323(2), 243–256 (2004).
196. Rosenfeld SJ, Yoshimoto K, Kajigaya S *et al.* Unique region of the minor capsid protein of human parvovirus B19 is exposed on the virion surface. *J. Clin. Invest.* 89(6), 2023–2029 (1992).
197. Ros C, Gerber M, Kempf C. Conformational changes in the VP1-unique region of native human parvovirus B19 lead to exposure of internal sequences that play a role in virus neutralization and infectivity. *J. Virol.* 80(24), 12017–12024 (2006).
198. Boschetti N, Niederhauser I, Kempf C, Stuhler A, Lower J, Blumel J. Different susceptibility of B19 virus and mice minute virus to low pH treatment. *Transfusion* 44(7), 1079–1086 (2004).
199. Yan Z, Zak R, Luxton GW, Ritchie TC, Bantel-Schaal U, Engelhardt JF. Ubiquitination of both adeno-associated virus type 2 and 5 capsid proteins affects the transduction efficiency of recombinant vectors. *J. Virol.* 76(5), 2043–2053 (2002).
200. Ros C, Kempf C. The ubiquitin-proteasome machinery is essential for nuclear translocation of incoming minute virus of mice. *Virology* 324(2), 350–360 (2004).
201. Suikkanen S, Aaltonen T, Nevalainen M *et al.* Exploitation of microtubule cytoskeleton and dynein during parvoviral traffic toward the nucleus. *J. Virol.* 77(19), 10270–10279 (2003).
202. Lombardo E, Ramirez JC, Garcia J, Almendral JM. Complementary roles of multiple nuclear targeting signals in the capsid proteins of the parvovirus minute virus of mice during assembly and onset of infection. *J. Virol.* 76(14), 7049–7059 (2002).
203. Vihinen-Ranta M, Wang D, Weichert WS, Parrish CR. The VP1 N-terminal sequence of canine parvovirus affects nuclear transport of capsids and efficient cell infection. *J. Virol.* 76(4), 1884–1891 (2002).
204. Cohen S, Marr AK, Garcin P, Pante N. Nuclear envelope disruption involving host caspases plays a role in the parvovirus replication cycle. *J. Virol.* 85(10), 4863–4874 (2011).
205. Cohen S, Behzad AR, Carroll JB, Pante N. Parvoviral nuclear import: bypassing the host nuclear-transport machinery. *J. Gen. Virol.* 87(Pt 11), 3209–3213 (2006).
206. Cohen S, Pante N. Pushing the envelope: microinjection of minute virus of mice into Xenopus oocytes causes damage to the nuclear envelope. *J. Gen. Virol.* 86(Pt 12), 3243–3252 (2005).
207. Cotmore SF, Hafenstein S, Tattersall P. Depletion of virion-associated divalent cations induces parvovirus minute virus of mice to eject its genome in a 3'-to-5' direction from an otherwise intact viral particle. *J. Virol.* 84(4), 1945–1956 (2010).
208. Cotmore SF, D'Abramo AM Jr, Ticknor CM, Tattersall P. Controlled conformational transitions in the MVM virion expose the VP1 N-terminus and viral genome without particle disassembly. *Virology* 254(1), 169–181 (1999).
209. Vanacker J-M, Rommelaere J. Non-structural proteins of autonomous parvoviruses: from cellular effects to molecular mechanisms. *Semin. Virol.* 6, 291–297 (1995).
210. Cotmore SF, D'Abramo AM Jr, Carbonell LF, Bratton J, Tattersall P. The NS2 polypeptide of parvovirus MVM is required for capsid assembly in murine cells. *Virology* 231(2), 267–280 (1997).
211. Eichwald V, Daeffler L, Klein M, Rommelaere J, Salome N. The NS2 proteins of parvovirus minute virus of mice are required for efficient nuclear egress of progeny virions in mouse cells. *J. Virol.* 76(20), 10307–10319 (2002).
212. Naeger LK, Salome N, Pintel DJ. NS2 is required for efficient translation of viral mRNA in minute virus of mice-infected murine cells. *J. Virol.* 67(2), 1034–1043 (1993).
213. Legrand C, Rommelaere J, Caillet-Fauquet P. MVM(p) NS-2 protein expression is required with NS-1 for maximal cytotoxicity in human transformed cells. *Virology* 195(1), 149–155 (1993).
214. Cotmore SF, Tattersall P. Parvovirus DNA replication. *Cold Spring Harbor Lab.* 799–813 (1996).
215. Riolobos L, Reguera J, Mateu MG, Almendral JM. Nuclear transport of trimeric assembly intermediates exerts a morphogenetic control on the icosahedral parvovirus capsid. *J. Mol. Biol.* 357(3), 1026–1038 (2006).
216. Lombardo E, Ramirez JC, Agbandje-McKenna M, Almendral JM. A beta-stranded motif drives capsid protein oligomers of the parvovirus minute virus of mice into the nucleus for viral assembly. *J. Virol.* 74(8), 3804–3814 (2000).
217. Cotmore SF, Tattersall P. A genome-linked copy of the NS-1 polypeptide is located on the outside of infectious parvovirus particles. *J. Virol.* 63(9), 3902–3911 (1989).
218. Reguera J, Grueso E, Carreira A, Sanchez-Martinez C, Almendral JM, Mateu MG. Functional relevance of amino acid residues involved in interactions with ordered nucleic acid in a spherical virus. *J. Biol. Chem.* 280(18), 17969–17977 (2005).

219. Chen KC, Shull BC, Lederman M, Stout ER, Bates RC. Analysis of the termini of the DNA of bovine parvovirus: demonstration of sequence inversion at the left terminus and its implication for the replication model. *J. Virol.* 62(10), 3807–3813 (1988).
220. Cotmore SF, Tattersall P. Encapsidation of minute virus of mice DNA: aspects of the translocation mechanism revealed by the structure of partially packaged genomes. *Virology* 336(1), 100–112 (2005).
221. Cotmore SF, Tattersall P. Genome packaging sense is controlled by the efficiency of the nick site in the right-end replication origin of parvoviruses minute virus of mice and LuIII. *J. Virol.* 79(4), 2287–2300 (2005).
222. Cotmore SF, Tattersall P. Mutations at the base of the icosahedral five-fold cylinders of minute virus of mice induce 3'-to-5' genome uncoating and critically impair entry functions. *J. Virol.* 86(1), 69–80 (2012).
223. Plevka P, Hafenstein S, Li L *et al.* Structure of a packaging-defective mutant of minute virus of mice indicates that the genome is packaged via a pore at a 5-fold axis. *J. Virol.* 85(10), 4822–4827 (2011).
224. Lang SI, Boelz S, Stroh-Dege AY, Rommelaere J, Dinsart C, Cornelis JJ. The infectivity and lytic activity of minute virus of mice wild-type and derived vector particles are strikingly different. *J. Virol.* 79(1), 289–298 (2005).
225. Kestler J, Neeb B, Struyf S *et al.* *cis* requirements for the efficient production of recombinant DNA vectors based on autonomous parvoviruses. *Hum. Gene Ther.* 10(10), 1619–1632 (1999).
226. Maroto B, Ramirez JC, Almendral JM. Phosphorylation status of the parvovirus minute virus of mice particle: mapping and biological relevance of the major phosphorylation sites. *J. Virol.* 74(23), 10892–10902 (2000).
227. Maroto B, Valle N, Saffrich R, Almendral JM. Nuclear export of the nonenveloped parvovirus virion is directed by an unordered protein signal exposed on the capsid surface. *J. Virol.* 78(19), 10685–10694 (2004).
228. Hernando E, Llamas-Saiz AL, Foces-Foces C *et al.* Biochemical and physical characterization of parvovirus minute virus of mice virus-like particles. *Virology* 267(2), 299–309 (2000).
229. Kanno H, Wolfinbarger JB, Bloom ME. Aleutian mink disease parvovirus infection of mink macrophages and human macrophage cell line U937: demonstration of antibody-dependent enhancement of infection. *J. Virol.* 67(12), 7017–7024 (1993).
230. Aasted B, Alexandersen S, Christensen J. Vaccination with Aleutian mink disease parvovirus (AMDV) capsid proteins enhances disease, while vaccination with the major non-structural AMDV protein causes partial protection from disease. *Vaccine* 16(11–12), 1158–1165 (1998).
231. Bloom ME, Martin DA, Oie KL *et al.* Expression of Aleutian mink disease parvovirus capsid proteins in defined segments: localization of immunoreactive sites and neutralizing epitopes to specific regions. *J. Virol.* 71(1), 705–714 (1997).
232. Porter DD, Larsen AE, Porter HG. The pathogenesis of Aleutian disease of mink. II. Enhancement of tissue lesions following the administration of a killed virus vaccine or passive antibody. *J. Immunol.* 109(1), 1–7 (1972).
233. Sato H, Hirata J, Kuroda N, Shiraki H, Maeda Y, Okochi K. Identification and mapping of neutralizing epitopes of human parvovirus B19 by using human antibodies. *J. Virol.* 65(10), 5485–5490 (1991).
234. Sato H, Hirata J, Furukawa M *et al.* Identification of the region including the epitope for a monoclonal antibody which can neutralize human parvovirus B19. *J. Virol.* 65(4), 1667–1672 (1991).
235. Brown KE, Cohen BJ. Haemagglutination by parvovirus B19. *J. Gen. Virol.* 73(Pt 8), 2147–2149 (1992).
236. Saikawa T, Anderson S, Momoeda M, Kajigaya S, Young NS. Neutralizing linear epitopes of B19 parvovirus cluster in the VP1 unique and VP1–VP2 junction regions. *J. Virol.* 67(6), 3004–3009 (1993).
237. Lopez-Bueno A, Mateu MG, Almendral JM. High mutant frequency in populations of a DNA virus allows evasion from antibody therapy in an immunodeficient host. *J. Virol.* 77(4), 2701–2708 (2003).
238. Kaufmann B, Lopez-Bueno A, Mateu MG *et al.* Minute virus of mice, a parvovirus, in complex with the Fab fragment of a neutralizing monoclonal antibody. *J. Virol.* 81(18), 9851–9858 (2007).
239. Chapman HN, Fromme P, Barty A *et al.* Femtosecond x-ray protein nanocrystallography. *Nature* 470(7332), 73–77 (2011).
240. Seibert MM, Ekeberg T, Maia FR *et al.* Single mimivirus particles intercepted and imaged with an x-ray laser. *Nature* 470(7332), 78–81 (2011).
241. Yu X, Ge P, Jiang J, Atanasov I, Zhou ZH. Atomic model of CPV reveals the mechanism used by this single-shelled virus to economically carry out functions conserved in multishelled reoviruses. *Structure* 19(5), 652–661 (2011).
242. Peng L, Ryazantsev S, Sun R, Zhou ZH. Three-dimensional visualization of gammaherpesvirus life cycle in host cells by electron tomography. *Structure* 18(1), 47–58 (2010).
243. Delano WL. The PyMOL Molecular Graphics System, Version 1.3, Schrödinger, LLC (2002).
244. Pettersen EF, Goddard TD, Huang CC *et al.* UCSF Chimera – a visualization system for exploratory research and analysis. *J. Comput. Chem.* 25(13), 1605–1612 (2004).
245. Xiao C, Rossmann MG. Interpretation of electron density with stereographic roadmap projections. *J. Struct. Biol.* 158(2), 182–187 (2007).